Task 4A/4B: Plans for Pile Instrumentation and Testing / Design Calculations and Specification for Piles

Evaluation of Glass Fiber Reinforced Polymer (GFRP) Spirals in Corrosion Resistant Concrete Piles

FDOT Contract Number: BDV30 977-27, FSU Project ID: 042924

Progress report date: 08/26/2020

(Initial submission to FDOT Structures Research Center: 11/26/2019, First revision: 06/23/2020)

Submitted to:

Florida Department of Transportation

Research Center

605 Suwannee Street

Tallahassee, Florida 32399-0450

Project Managers:

Christina Freeman	FDOT Structures Research Center
Ge Wan	FDOT Structures Design Office
Rodrigo Herrera	FDOT Structures Design Office

FAMU-FSU Engineering

Prepared by:

Olayiwola Adegbulugbe	Graduate Research Assistant
Sungmoon Jung	Principal Investigator
Raphael Kampmann	Co-Principal Investigator

Department of Civil and Environmental Engineering

FAMU-FSU College of Engineering

2525 Pottsdamer St., Tallahassee, FL. 32310.

TABLE OF CONTENTS

Chapter 1. Introduction........6

Chapter 2. Instrumentation and Testing Plan........7

2.1 Introduction........7

2.2 Instrumentation........7

2.2.1 Strain Gauges........7

2.2.2 Deflection Gauges........8

2.2.3 Fiber Optic Gauges........8

2.2.4 Vibrating Wire Gauges........8

2.2.5 Accelerometers........9

2.2.6 Pile Driving Analyzer® (PDA)........11

2.2.7 Infrared Optical Break Beam Sensors........12

2.2.8 High-speed Cameras........12

2.3 Procedures for Instrumentation........13

2.3.1 Procedures Prior to Casting........13

2.3.2 Post-casting Procedures........13

2.3.3 Pre-impact Setup Procedures........14

2.4 Procedure for Testing........16

2.4.1 Procedure for Impact Tests........16

2.4.2 Procedure for Flexural and Axial Tests........20

Chapter 3. Design Calculation and Construction Plans........21

3.1 Introduction........21

3.2 Design Calculations for the Spiral Size........21

3.2.1 Selection of GFRP Spiral Size........21

3.2.2 Size of CFRP and GFRP Spiral Based on Equivalent Steel Spiral Tensile Capacity and FRP Strain Limit 22
3.2.3 Size of CFRP and GFRP Spiral Based on Equivalent Steel Spiral Shear Capacity 23
3.3 Specification for GFRP Spirals 24
3.4 Design Calculations for Testing Related Properties 25
3.4.1 Prestress Loss Calculations 25
3.4.2 Moment Capacity Calculations 26
3.4.3 Axial Capacity Calculations 26
3.4.4 Flexural Displacement Calculations 27
3.4.5 Comparison of Results based on Design Concrete Properties and Expected As-built Concrete Properties 27
Bibliography 30
Appendices 32
Appendix A Instrumentation Plan 32
A1 Pile Information 33
A2 Instrumentation Numbering 34
A3 Tests and Sensors Monitored 35
A4 Internal (Spiral) Strain Gauge and Fiber Optic Gauge Instrumentation for PSS 39
A5 Internal (Spiral) Strain Gauge and Fiber Optic Gauge Instrumentation for PSG1 . 40
A6 Internal (Spiral) Strain Gauge, Fiber Optic Gauge and Vibrating Wire Instrumentation for PSG2 41
A7 Axial Test Setup 44
A8 Flexural Test Setup/Instrumentation 45
A9 Cable Routing for Internal Instrumentation 47
A10 PDA Instrumentation 48
Appendix B Data Sheet for EGCS-D5 Accelerometer 49

Appendix C Impact Test Setup 54

Appendix D Size of CFRP and GFRP Spiral Based on Force Equilibrium......................... 56

Appendix E Prestress Loss Calculations 59

Appendix F Moment Capacity Calculations 65

Appendix G Calculations for Axial Capacities and Compression Driving Stress Limits.... 68

Appendix H Calculations for Flexural Displacement 71

Appendix I Calculations for Shear Capacity of Transverse Reinforcement 76

LIST OF FIGURES

Figure 2.1: Pile acceleration from finite element impact analysis (filtered data). 9
Figure 2.2: Pile acceleration from finite element impact analysis (raw data).....................................10
Figure 2.3: Location of break beams (elevation). 12
Figure 2.4: Strand cutting sequence. 14
Figure 2.5: Pile cushion with screw eyes. 15
Figure 2.6: Pile cushion placement (McVay et al., 2009)..16
Figure 2.7: Top stress prediction based on impactor drop height. 17
Figure 2.8: Estimated displacement. 18

LIST OF TABLES

Table 1.1: Pile nomenclature in the report....6
Table 2.1: Distinguishing characteristics of strain gauges used....8
Table 3.1: Required area of transverse reinforcements compared to the prescribed area....23
Table 3.2: Comparison of the shear capacity of transverse reinforcement....24
Table 3.3: Physical and mechanical property requirements for GFRP spirals....24
Table 3.4: Geometric and mechanical properties requirement for GFRP bars....25
Table 3.5: Comparison of results based on design vs. expected as-built concrete strength....29

Chapter 1. Introduction

To evaluate the GFRP spiral reinforcement in prestressed concrete piles, the first phase of this research will test four 30 ft.-long prestressed concrete piles with a cross section of 24 in. × 24 in. The first pile is the control specimen composed of steel strands and steel spirals. It is based on the FDOT's standard details for a 24-inch square prestressed concrete pile. The next two piles have steel strands and GFRP spirals. In addition, one pile with CFRP strands and spirals from a previous project (Roddenberry et al., 2014) will also be tested. The drawings of the piles are shown in Appendix A1. The nomenclature given in Table 1.1 is used throughout this report.

Table 1.1: Pile nomenclature in the report

Pile Label	Strand Type	Spiral Type	To Be Casted	Note
PSS	Steel	Steel	Yes	Control specimen
PSG1 PSG2	Steel	GFRP	Yes	One for impact; the other for axial & bending
PCC	CFRP	CFRP	No	Pile from a previous project

Pile nomenclature is such that the first letter 'P' represents 'pile'. The second letter represents the type of longitudinal reinforcement. The last letter represents the type of spiral used. 'S' is for steel, 'G' is for GFRP bars and 'C' is for CFRP bars. For example, PSG is a pile with steel longitudinal reinforcement and GFRP spirals.

Chapter 2 discusses the procedures for the instrumentation of the piles both before casting and after casting, as well as the procedures to follow during the testing. Chapter 3 presents the calculations for the design, specifications for GFRP spirals and prediction of pile behavior.

Chapter 2. Instrumentation and Testing Plan

2.1 Introduction

In this chapter, the instrumentation for obtaining data at various stages of pile test, both at the casting yard and at FDOT Structures Research Center is described. Also, the procedures for installing the instrumentation and the procedures for conducting the various pile experiments are given.

2.2 Instrumentation

Tests in this study includes impact tests, a flexural test, and axial tests. The instrumentation to collect data from the tests includes strain gauges, deflection gauges, fiber optic gauges, vibrating wire gauges, accelerometers, Pile Driving Analyzer® (PDA), infrared optical break beam sensors and high-speed cameras. The notation and numbering for the instrumentation are shown in Appendix A2.

2.2.1 Strain Gauges

External concrete strain and internal spiral strain measurements will be taken for tests in this study. Therefore, three models of strain gauges, manufactured by KYOWA Electronic Instruments, will be used. For external concrete strain measurements, the model KC-60-120-A1-11 wire strain gauges will be used, whereas for the internal spiral strain measurements two models; KFGS-5-120-C1-11 and KFRPB-5-120-C1-9 foil strain gauges will be used for the steel spiral and GFRP spiral, respectively. The difference in strain gauge model for spiral strain measurements is to ensure the gauges are compatible with the materials to be evaluated, namely the steel and GFRP spirals. According to the manufacturer, the KFRPB model series has a special gauge pattern that minimizes the effect of self-heating due to gauge current and the effect of reinforcement of low elasticity. While all three gauges have a resistance of 120 Ω, their distinguishing characteristics are summarized in Table 2.1. The layout of the external gauges (KC-60-120-A1-11) are shown in Appendix A8 (second page) while the layout for internal gauges (KFGS-5-120-C1-11 and KFRPB-5-120-C1-9) are as shown in Appendix A4, A5, and A6 (second page).

Table 2.1: Distinguishing characteristics of strain gauges used

Strain Gauge Model	Gauge Length/width mm	Backing Length/width mm	Linear Expansion Coefficients $\times 10^{-6}/^{o}C$
KC-60-120-A1-11	60/0.6	74/8	11
KFGS-5-120-C1-11	5/1.4	9.4/2.8	11
KFRPB-5-120-C1-9	5/1.4	15/5	9

2.2.2 Deflection Gauges

The deflection of PSG2 during the flexural test will be measured by non-contact laser deflection gauges provided by the FDOT Structures Research Center. These deflection gauges can project lasers in areas where contact deflection gauges cannot reach. Also, in areas where the spreader beam is above the top face of the specimen as shown in Appendix A8, lasers from defection gauges are projected on 2 in. angles glued to the top side of the specimen to avoid interference with the spreader beam (Roddenberry et al., 2014). Non-contact laser deflection gauges are easy to install. Appendix A8 provides details on the layout of the deflection gauges used.

2.2.3 Fiber Optic Gauges

Fiber optic strain gauges will be installed on all three (3) piles that will be made at the precast yard. The gauges will be embedded at both ends of the piles. To facilitate the embedment of the gauges, six 42-in.-long GFRP bars will be machined to creates grooves in which the fiber optic gauges will be bonded. The fiber optic gauges will provide a means of monitoring stress changes in the pile when prestressing strands are de-tensioned. In addition, fiber optic gauges in PSG2 will be re-connected during axial testing for axial strain measurements. The layout of the Fiber optic gauges are shown in Appendix A4 to A6.

2.2.4 Vibrating Wire Gauges

Prior to concrete placement in PSG2, a total of eight Geokon Model 4200 vibrating wire strain gauges will be installed in the pile. The layout of vibrating wire placement is shown in Appendix A6. Geokon Model 4200 vibrating wire strain gauges have a gauge length of 6-in., a nominal range of 1,000 $\mu\varepsilon$ to 4,000 $\mu\varepsilon$, a resolution of 1 $\mu\varepsilon$ and an operational temperature range of -4 °F to 176 °F (-20 °C to 80 °C). A Geokon GK-404 manual readout will be used to obtain strain measurements from the vibrating wires during axial testing. These measurements will be compared to axial strain measurements from the fiber optic gauges described in Section 2.2.3.

2.2.5 Accelerometers

To measure acceleration and indirectly quantify impact force during the impact event, accelerometers will be mounted externally on the impactor and the pile under investigation in the direction of impact. On the impactor, an accelerometer is mounted at the center of the top face of the impactor, while on the pile, an accelerometer is mounted on the side of the pile at 3 ft., from the pile head (Appendix A10). According to ASTM D4945-17, the transducers should be located at a distance of at least 1.5 times the width of the pile from the pile toe and/or the pile top. This location is such that irregular stress concentrations at the ends of the pile can be avoided during data collection. Also, the finite element analysis carried out in Task 2A supports the accelerometer placement at 3 ft. from the pile top as shown in Figure 2.1. The measurement at 3 ft. from the pile top will provide another data point for research purposes since the PDA accelerometers will obtain measurement at 4 ft. from the pile head as discussed in Section 2.2.6.

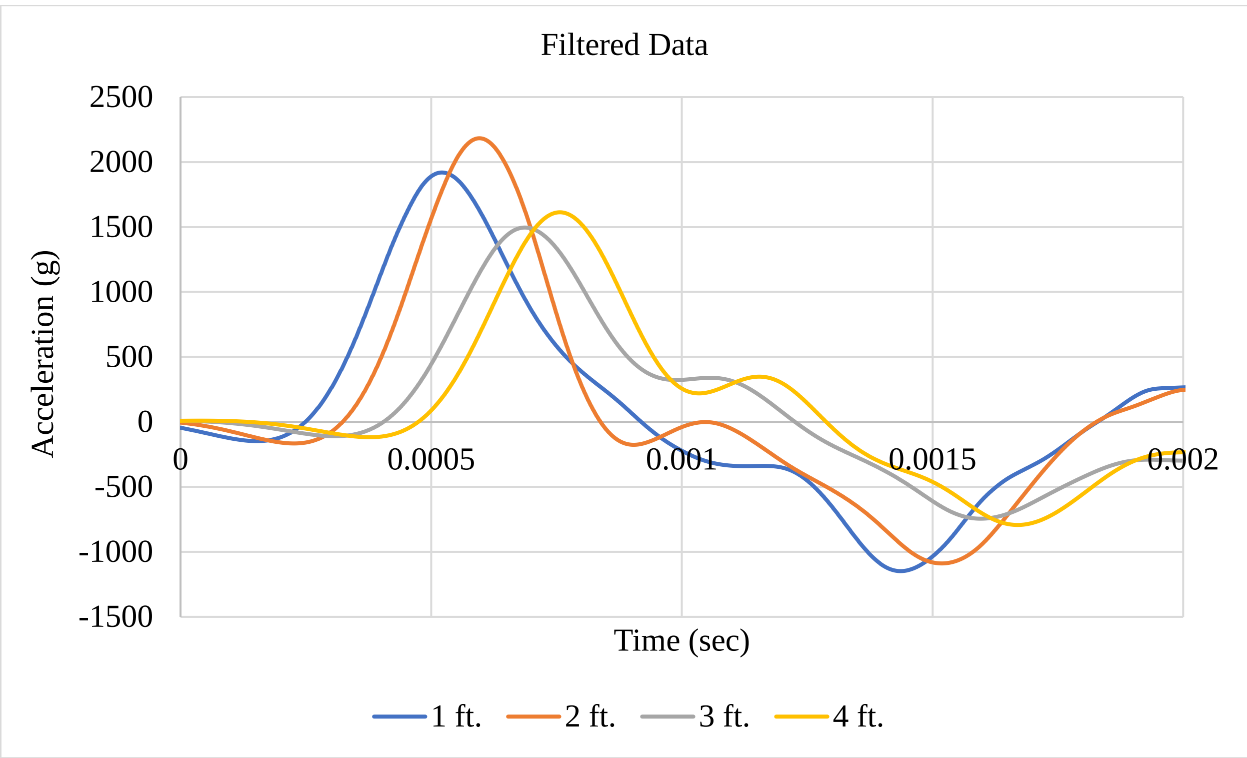

Figure 2.1: Pile acceleration from finite element impact analysis (filtered data).

The processed analysis output in Figure 2.1 shows initial negative acceleration, which can be attributed to the Channel Frequency Class (CFC) 1000 filter that was applied to the raw data output shown in Figure 2.2. However, the magnitude of the negative acceleration with respect to the peak acceleration is small (an average of 7.5 %). The raw data shows that the acceleration is positive initially, but it suffers from the numerical noise. The standard practice is to apply the filter to remove the noise that is not physically meaningful. The CFC 1000 is the highest filter class, meaning that it preserves the most high-frequency content than other CFC filter classes. The cut-off frequency of CFC 1000 filter is 1.65 kHz.

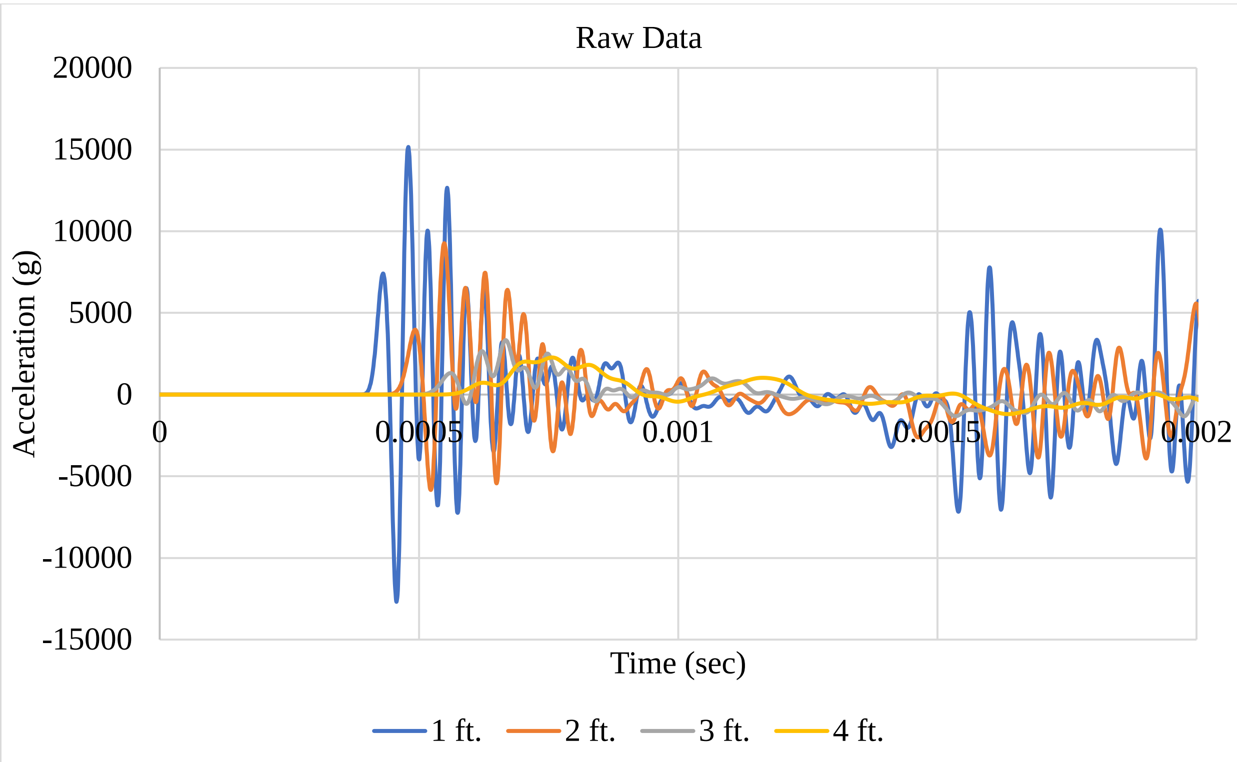

Figure 2.2: Pile acceleration from finite element impact analysis (raw data).

Also, based on acceleration results obtained from numerical impact analysis, the accelerometers to be mounted on the impactor and on the pile (at 3 ft. from the pile top) will be model EGCS-D5 accelerometers by TE connectivity. These accelerometers have a measurement range of ±5,000 g and a shock limit of 20,000 g. To ensure accurate measurements from the accelerometers, they will be calibrated by TE connectivity over their respective cable length. The data sheets for the accelerometers are provided in Appendix B.

The following are the methods and procedures for attaching the EGCS-D5 accelerometers to the pile and the impactor.

1. An EGCS-D5 accelerometer will be attached to the pile using an adhesive anchor system. The adhesive anchor system will utilize the bonding mechanism between the adhesive and the anchor element, and the adhesive and the concrete, to transfer acceleration responses. The system will be setup as follows: a) Measure and mark 3 ft. on the side of the pile starting from pile top along the center. b) Drill holes 0.38 in. apart, center to center, along the marked line on either side of the centerline. Each hole should have a depth of 2 in. and should fit a #4-40 unc class 2B threaded rod with adhesive. c) remove dust from each hole by blowing with compressed air. d) clean each hole with steel brush and remove dust from holes again by blowing with compressed air. e) Fill the first hole ½ way with epoxy starting from the bottom. f) Insert clean anchor (3 in.-long 4-40 threaded rod) into the hole, turning slowly until it reaches the bottom of the hole. g) Allow to fully cure. h). Repeat steps d to g for the second hole. i) Place accelerometer and secure with flanged nuts.
2. An EGCS-D5 accelerometer will be screw mounted on top of the impactor. Accelerometer location will be at the center of the impactor in longitudinal and transverse directions. The accelerometer will be installed as follows: a) Drill/tap the top steel plate of the impactor to create holes that are 0.38 in. apart, center to center, such that the accelerometer's center of mass coincides with the center of mass of the impactor along the axis of impact. Each hole should have a depth of 1 in. and should fit a #4-40 unc class 2B screw. b) Ensure a smooth and flat machined surface for attaching the accelerometer and clean the area to ensure that metal burrs and other foreign particles do not interfere with the contacting surfaces. c) For the best high-frequency transmissibility, apply a thin layer of silicone grease between the accelerometer base and the mounting surface. d) Place accelerometer and secure with screws.

2.2.6 Pile Driving Analyzer® (PDA)

Piles PSS, PSG1 and PCC will be monitored using the Pile Driving Analyzer® (PDA) during impact events. For this project, the PDA system consists of strain transducers and accelerometers mounted close to the pile top and pile toe, to measure the axial stress induced by the impactor. In this research, in accordance with ASTM D4945-17, the PDA instrumentation will be located at 4 ft. from both ends of the pile as shown in Appendix A10. This location was chosen to avoid local contact stresses at the ends of the pile based on recommendations from the contractor providing the PDA instrumentation (Terracon Consultants, Inc.).

2.2.7 Infrared Optical Break Beam Sensors

Infrared optical break beam sensors will be installed to quantify pendulum speed close to the point of impact as shown in Figure 2.3. For this measurement, two sensor pairs each consisting of a transmitter and receiver will be mounted on aluminum stands (see Figure 2.3). One pair of sensors will be located near the impact point and the other pair will be located 1 ft. away from the first pair. From the distance between the sensors, and the duration between infrared beam interruptions, the speed of the impactor just before hitting the cushion at the pile head can be determined. All sensors will be positioned at a level corresponding to the mid-height of the impactor at the bottom of the swing.

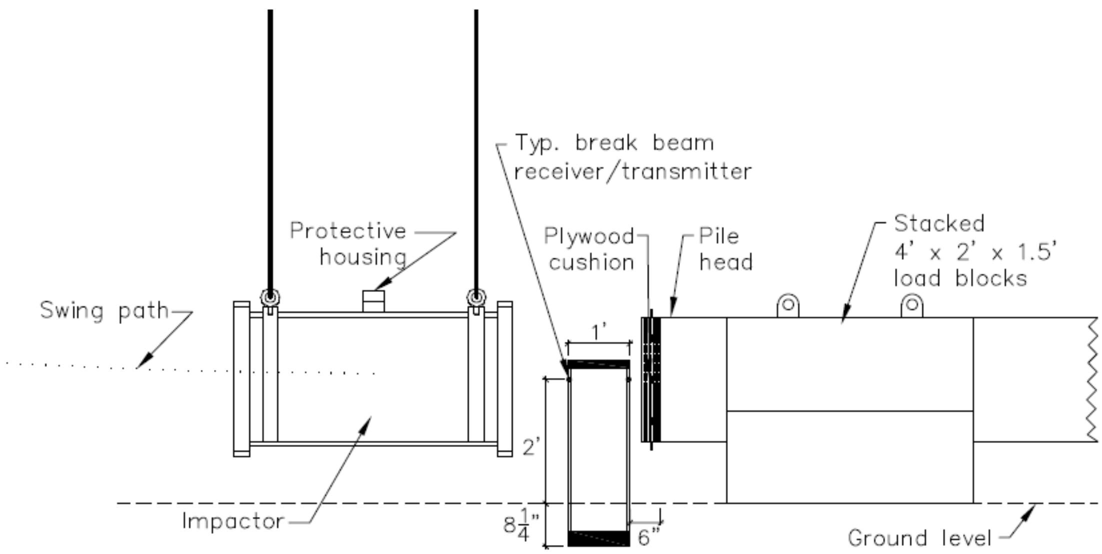

Figure 2.3: Location of break beams (elevation).

2.2.8 High-speed Cameras

In addition to the experimental instrumentation provided, the impact event will be captured on two high-speed video cameras. The high-speed camera recordings will be triggered when the impactor passes by the break beams. These cameras will provide another means of estimating the speed of the impactor just before impact. Therefore, one of the cameras will produce an up-close side elevation of the impact event, while the second camera will produce a wide-angle view of the impact experiment. Each camera has a recording rate of 2,000 frames/second.

2.3 Procedures for Instrumentation

2.3.1 Procedures Prior to Casting

1. The spiral reinforcements for the piles shall be brought to the FDOT Structures Laboratory for necessary instrumentation.
2. Install fiber optic gauges bonded within groves that machined on 42-in.-long GFRP bars at both ends of PSS, PSG1 and PSG2.
3. Install vibrating wire gauges within the spiral cage (of PSG2), as shown in Appendix A6, by using GFRP bars and polystyrene foams to offset vibrating wire gauges from spirals. This offset is to prevent the interference between spirals the coil assembly of the vibrating wire gauges. The orientation of the vibrating wire gauges is longitudinal, i.e., parallel to the strands.
4. Install strain gauges. a) Mark area of spiral to be gauged for spiral strain measurements as shown in Appendix A4 to A6 for PSS, PSG1 and PSG2. b) Carefully grind/smoothen bar surface for gauge installation. Clean bar surface with acetone for satisfactory bond of gauges to the reinforcement. c) Attach strain gauges to the spirals as shown in Appendix A4 to A6. Avoid contaminating the bonding surface of the gauges while attaching the gauges. d) Ensure that the gauges are protected from moisture and mechanical damage. Protect wires by using zip ties, such that no damage occurs in case wires are pulled during concrete casting. e) Check that gauges are functioning normally and replace any malfunctioning gauge.
5. Label all gauge wires and bundle them together using ties. The wires must extend outside the concrete volume prior to casting. The cables within the pile should be routed as shown in Appendix A9. The set of cables for the first 10 spiral turns for PSS and PSG1, should be bundled separately from the other cables. This is because the pile will be cut at some point during the impact test, and readings will be obtained for the gages close to the cutoff point. Therefore, these cables need to be intact after cutting the pile.
6. Deliver the instrumented spiral reinforcements to the pre-caster.

2.3.2 Post-casting Procedures

1. De-tension strands and record fiber optic gauge responses. The fiber optic gauges will be used to monitor strains in the concrete as the strands are cut and stresses are transferred from the strands to the concrete. The pile cylinder strength shall be at least 4000 psi at the

time of transfer of prestressing force. Monitor the fiber optic gauges throughout the de-tensioning process at a data recording rate of 20 Hz following these steps. a) Record base line fiber optic gauge reading prior to de-tensioning. b) Cut prestressing strands in a symmetrical cutting sequence using the flame cutting technique. A similar cutting sequence was used by Roddenberry et al. (2014) as shown in Figure 2.4. To avoid sudden stress transfer when flame cutting prestressing strands, strands shall be cut with a sweeping motion with a minimum sweep of 3 inches side to side (6 inches total) along the direction of the strand. c) Stop monitoring the fiber optic gauges 30 minutes after the de-tensioning process has been completed.

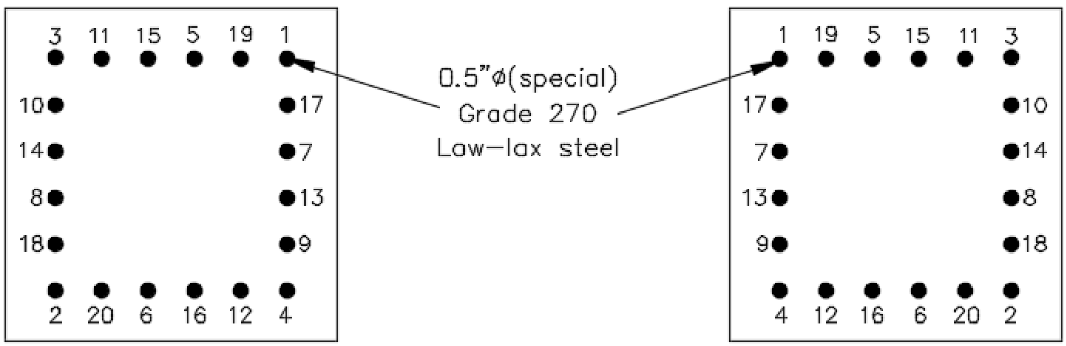

a. Live end *b. Dead end*

Figure 2.4: Strand cutting sequence.

2. For PSS and PSG1, mechanically cut strands flush with the concrete surface and mark the pile to identify the top end. However, for PSG2 do not cut strands flush with the concrete surface. Instead leave at least 3 in. of strands at both ends.

2.3.3 Pre-impact Setup Procedures

For impact testing, a pendulum impactor suspended by cables will swing in a circular path when released from a certain drop height. For the first test swing, a drop height of 2 ft. will be used to estimate the force delivered to the pile top. Based on the force and stress estimates from the first test swing, a second drop height, which can deliver 3.5 ksi at the top of the pile will be recommended on site. Also, based on the force and stress estimates from the two previous test swings, a third drop height, which can deliver 5 ksi at the top of the pile will be recommended on site. Finally, the drop height of the impactor will be set at 18 ft. to perform the last impact test for a pile. However, before any of the aforementioned swings are conducted, set up the pile, restraints, and support as described in Appendix C. On the impactor, mount an EGCS-D5 accelerometer at the center of the top face of the impactor as described in Section 2.2.5. Then, suspend the impactor by cables attached to the pylons. Subsequently, take the following steps:

1. Attach plywood pile cushions to the pile top and the pile toe. a) Make plywood pile cushion to be used at the pile top and the pile toe into desired thicknesses by gluing multiple plywood, each having a nominal thickness of 3/4 in. The starting cushion thickness shall be 4.5 in. at the pile top and 1.5 in. at the pile toe for a low drop height (2 ft.). If needed the cushion thickness shall be varied for subsequent drop heights. b) Insert screw eyes along the sides of the plywood cushion as shown in Figure 2.5. For multiple layers of plywood cushion, insert the screw eyes at the center line or close to the center line of the cushion. c) Create four corner grooves, 1.5 ft. from the pile top and the pile toe. Attach ropes (or steel wires) strongly such that it passes through the four grooves in a transverse direction. d) Attach cushions at the pile top and pile toe with ropes (or steel wires) that run longitudinally from the screw eyes on the sides of the cushion to the transverse ropes 1.5 ft. from the pile top and the pile toe as seen in Figure 2.6.

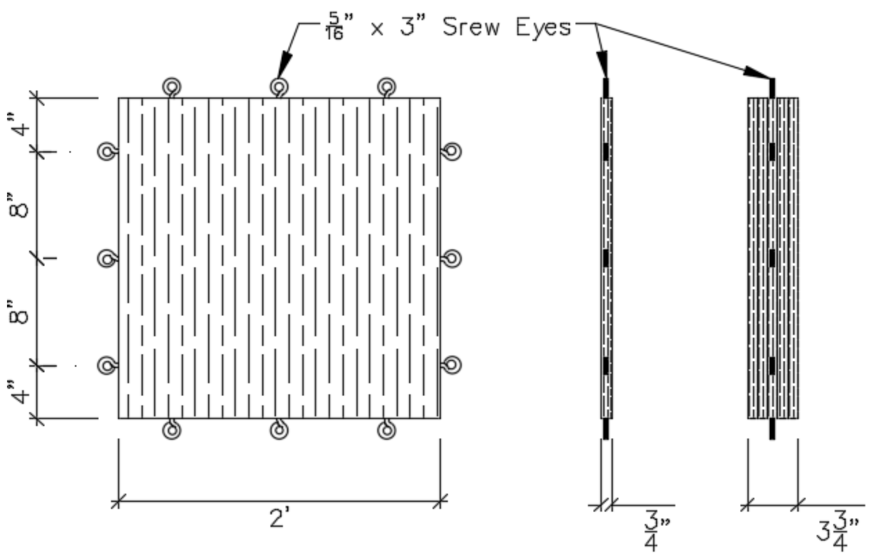

a. Front view *b. Side view (different thicknesses)*

Figure 2.5: Pile cushion with screw eyes.

Figure 2.6: Pile cushion placement (McVay et al., 2009).

2. Set up the sensors. Mount EGCS-D5 accelerometer on pile as described in Section 2.2.5. Install infrared optical break beam sensors as described in Section 2.2.7. Connect all sensors (strain gauges, EGCS accelerometer and infrared optical break beam sensors) to the data acquisition system.
3. Install PDA accelerometers and transducers on the pile surface as shown in Appendix A10. This will be done by the PDA personnel from Terracon Consultants, Inc.
4. In addition to the experimental instrumentation provided, the impact event will be captured on two high-speed video cameras. One camera should produce an up-close side elevation of the impact event, while the second camera should produce a wide-angle view of the impact experiment. Each camera will record at a rate of 2,000 frames/second.

2.4 Procedure for Testing

2.4.1 Procedure for Impact Tests

For each pile to be tested under impact loading, four different test swing will be performed. The first test swing will be performed at a low drop height of 2 ft. Based on the force and stress estimates from the first test swing, a second drop height that can deliver 3.5 ksi at the top of the pile will be recommended on site. Also, based on the prior stress estimates a third drop height that can deliver 5 ksi will be recommended on site. Figure 2.7 shows the current stress prediction at the pile top depending on the drop height of the impactor. Figure 2.7 was obtained using 0.7 as the coefficient of restitution (C_R). This value was obtained from the finite element analysis that was carried out in Task 2A. The coefficient of restitution, defined in Equation (2.1), is a measure of the kinetic energy dissipation between the impactor and the pile. From the first test swing, the appropriate coefficient of restitution will be determined using the velocity measurements (after processing the acceleration responses), then the drop height to achieve a top stress of 3.5 ksi will be determined.

$$C_R = \frac{v_{bf} + v_{af}}{v_{ai}} \tag{2.1}$$

where v_{ai}, v_{af}, and v_{bf} are the velocity of the impactor just before the impact, velocity of the impactor after the impact, and velocity of the pile after the impact, respectively.

For third test swing, parameters determined and verified from the first two test swings will be used to determine the drop height to achieve a top stress of 5 ksi.

Finally, a fourth test swing for the pile is performed at a drop height of 18 ft, which based on current prediction, will result in a top stress of 7.7 ksi as shown in Figure 2.7.

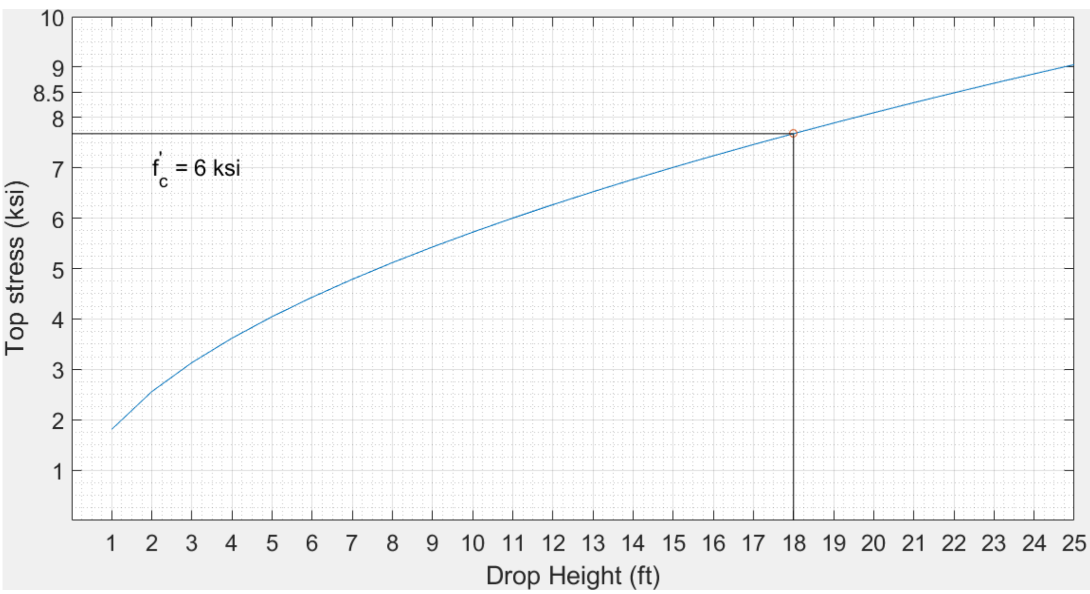

Figure 2.7: Top stress prediction based on impactor drop height.

For each test swing, the data acquisition system, except the high-speed cameras, shall be turned on just before the impactor is released and all sensor responses shall be recorded at 10,000 samples/sec (10 kHz). The high-speed camera recordings will be triggered when the impactor passes by the break beams. The duration of data recording shall be 10 seconds (starting from the release of the impactor) under each test swing to sufficiently capture data. Stress and strain measurements from the PDA instrumentation will only be monitored and recorded for the first three test wings because it is assumed that the fourth test will damage the pile. For that reason, the PDA gauges will be disconnected to avoid damaging them. See Appendix A3 (second page) for sensors monitored during this test.

At the end of each swing, the restraining blocks at the pile toe would have been displaced. The estimated range of displacement based on assumed friction coefficients (0.3, 0.4 and 0.5) for various drop heights is shown in Figure 2.8. This is a rough estimate because the friction coefficient (μ) at the site was not measured. However, based on the work energy theorem, the coefficient of friction (μ) at the site can be determined after the first test as shown Equation (2.2).

$$m_c g \mu d = \frac{1}{2}(m_b + m_c)v_{bf}^2 \tag{2.2}$$

where m_b, m_c, g and d are the approximate mass of the pile, approximate mass of the restraints block, acceleration due to gravity and the measured displacement at the pile toe, respectively.

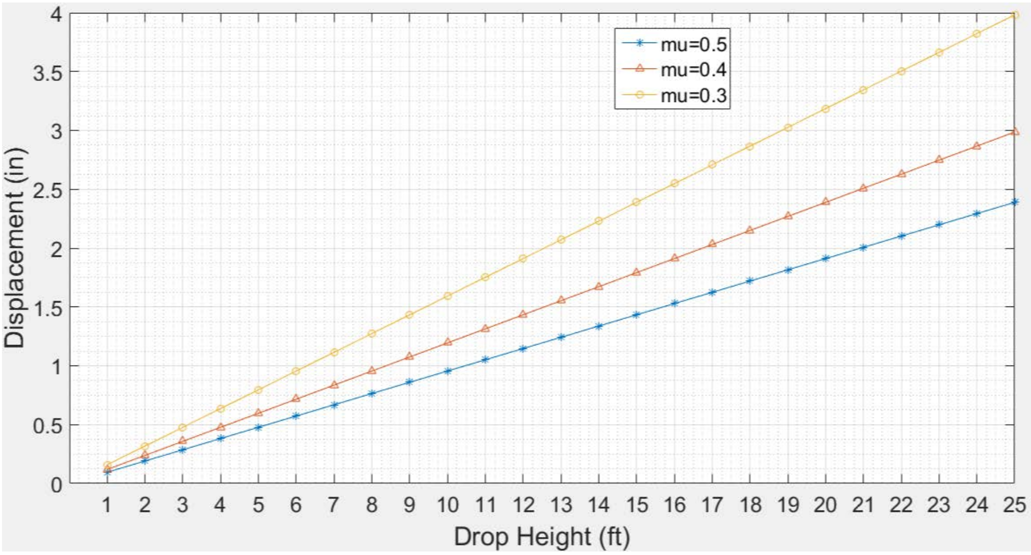

Figure 2.8: Estimated displacement.

The restraining blocks will be repositioned as soon as displacement exceeds 12 in., therefore, an exact estimate of the displacement is not necessary.

The summary of the procedures for impact testing is as follows:

1. Starting with the control specimen (PSS), raise the impactor to an initial drop height of 2 ft. Release impactor and allow it to hit the pile. Record the measured responses.
2. Determine the velocity of the impactor just before and after impact, and the velocity of the pile after impact by integrating the acceleration responses. Using the velocities calculated, determine the coefficient of restitution (C_R) using Equation (2.1).
3. Measure the displacement of restraining blocks at the end of the pile with a tape measure. Using the displacement value, determine the coefficient of friction (μ) using Equation (2.2).
4. Using the coefficient of restitution and coefficient of friction determined in step 2 and step 3, determine the drop height at which the impactor will deliver a stress of 3.5 ksi at the pile top.
5. Reposition pile and restraining blocks by using a crane if the displacement from the initial starting position reaches or exceeds 12 in.
6. Raise the impactor to the drop height determined in step 4. Release impactor and allow it to hit the pile. Record the measured responses.
7. Repeat Steps 4-6 but to deliver the stress of 5 ksi.
8. Again, reposition pile and restraining blocks by using a crane if the displacement from the initial starting position reaches or exceeds 12 in.
9. Disconnect PDA instrumentation to avoid being damaged by the next test swing.
10. Raise the impactor to a drop height of 18 ft. Release impactor and allow it to hit the pile. Record the measured responses.
11. After completing the four test swings (at 2 ft., height resulting in 3.5 ksi, height resulting in 5 ksi and 18 ft.), disconnect all gauges except S21 to S24 (or S73 to S76 for PSG1) from the data acquisition system.
12. With strain gauges S21 to S24 (or S73 to S76 for PSG1) still connected to the data acquisition system, cut the pile as would be done in the field at 2.5 ft from the pile top. The cutting of the pile will be contracted to Great Southern Demolition Inc. After cutting the pile as described, monitor strains in the gauges close to the cutoff location.
13. Repeat steps 1 to 12 for PSG1.
14. Repeat steps 1 to 10 for PCC. Disconnect all gauges from the data acquisition system after performing the test.

2.4.2 Procedure for Flexural and Axial Tests

1. Setup the experiment as described in Appendix A8 for PSG2. Check gauges to ensure they are in good condition and replace malfunctioning gauges.
2. Apply load at a rate of 250 pounds per second until the first flexural cracks are noticed. Afterwards, change load rate to 200 pounds per second. Record data at 10 samples/sec (10 Hz).
3. Intermittently mark and sketch crack patterns. Mark cracks at the predicted actuator cracking load (approximately 33 kips, as explained in Section 3.4.4) and at 55 kips actuator load which is approximately 53 % of the max actuator load.
4. Continue test until failure occurs, then unload the pile. The predicted flexural displacement at failure is 3.88 in.
5. Cut the pile at 6 ft. from both ends and use the end specimens obtained for the axial tests. Setup the axial tests as shown in Appendix A7. Connect gauges to the data acquisition system.
6. Apply load at a rate of 250 pounds per second until the actuator load reaches 500 kips. Record and monitor live readings at 10 Hz. Perform axial tests on the two specimens shown in Appendix A7 and obtain longitudinal and transverse strain readings.

Chapter 3. Design Calculation and Construction Plans

3.1 Introduction

The design of the control specimen – PSS – will follow the FDOT standard plans for 24-inch square prestressed concrete pile, which recommends W3.4 steel spiral ties (with a cross sectional area of 0.034 in.^{2}). In this project, a 24-inch CFRP prestressed concrete pile, which has 0.2-inch diameter CFRP spiral ties based on the FDOT standard plans, will also be tested Therefore, this section will focus mainly on the GFRP spiral size selection for PSG1 and PSG2 (see Table 1.1 for the pile nomenclature). However, to facilitate the discussion, the CFRP spiral size will also be discussed even though a new CFRP pile will not be casted in this project.

3.2 Design Calculations for the Spiral Size

3.2.1 Selection of GFRP Spiral Size

The current FDOT design requirements for the steel spirals in prestressed concrete piles are prescriptive based on years of successful practice rather than from an analytical calculation. Therefore, the approaches below will select the GFRP spiral size that provides the same performance as the steel spiral (as proven by years of successful practice). To ensure the selection of the correct spiral size, two different approaches will be used as shown in Sections 3.2.2 and 3.2.3.

Again, the proposed design is to select a GFRP spiral size that matches the performance of the successful steel spiral provided by FDOT. Therefore, we are not following Article 5.6.4.6 of AASHTO (2017), because it is too conservative for piles. It is too conservative because it assumes complete failure/spalling of the outer concrete while maintaining the load carrying capacity of the pile using the core of the concrete alone. Also, compression members designed as piles follow specifications for non-pile compression members. This is because piles might be required to protrude from the soil. Also, when fully embedded in the soil, it is uncertain that the surrounding soil will sufficiently support the entire length of the pile to prevent lateral bukling (Graybeal & Pessiki, 1998). For reference purposes, this conservative approach is given in Appendix D

3.2.2 Size of CFRP and GFRP Spiral Based on Equivalent Steel Spiral Tensile Capacity and FRP Strain Limit

The first approach in determining the required area of FRP spiral is to compare the tensile capacity of steel spiral to the tensile capacity of FRP transverse reinforcement. This approach utilizes the demonstrated success of the FDOT steel spiral design based on the years of experience. The tensile capacity of the steel spiral is calculated below as the product of its yield stress and area. The properties of the steel spiral prescribed for a 24-inch square prestressed concrete pile are as follows:

Area of steel spiral, $A_s = 0.034$ in.^{2}

Minimum tensile stress, $f_u = 80$ ksi

Minimum yield stress, $f_{yh} = 70$ ksi (ASTM A1064-18a)

Therefore, the tensile capacity of the steel spiral is

$$F_{steel} = A_s f_{yh} \tag{3.1}$$

$$F_{steel} = 70 \text{ ksi } (0.034 \text{ in.}^2) = 2.38 \text{ kips}$$

Next, the required FRP spiral area was computed using the force equivalency. Unlike steel, FRP does not have clear yield stress, and ultimate stress should not be reached to prevent brittle failure. Instead of using the stress value directly, it was computed using the elastic modulus and a strain limit. According to ACI 440.1R-15, the effective strain in FRP reinforcement should not exceed 0.004 to avoid degradation of aggregate interlock, control shear crack widths and prevent concrete shear. However, we are providing confinement with the end spirals not transverse shear, therefore, a higher strain limit of 0.006 was utilized as recommended by CSA-806. With this strain limit and the modulus of elastic of the FRP, the area of FRP rebar that provides a tensile capacity equivalent to that of the standard steel spiral was obtained as follows:

Modulus of Elasticity of CFRP, $E_{CFRP} = 22400$ ksi (pending requirements in FDOT specifications 932-3)

Modulus of Elasticity of GFRP, $E_{GFRP} = 6500$ ksi (ASTM D7957-17)

$$\text{Area of FRP required, } A_{FRP} = \frac{F_{steel}}{\varepsilon E_{FRP}} \tag{3.2}$$

where A_{FRP}, ε, and E_{FRP} are the required area, effective strain, and modulus of elasticity of the FRP reinforcement, respectively. Therefore,

Area of CFRP required, $A_{CFRP} = \frac{2.38}{(0.006)(22400)} = 0.018$ in.^{2}

Area of GFRP required, $A_{GFRP} = \frac{2.38}{(0.006)(6500)} = 0.061 \text{ in.}^2$

Table 3.1 below shows the required area of CFRP and GFRP transverse reinforcement based on the calculation above, as well as the area of CFRP transverse reinforcement prescribed by Roddenberry et al. (2014) and the newly prescribed area of GFRP transverse reinforcement. The #3 GFRP rebar is prescribed, which has a nominal diameter of 0.375 in. and cross-sectional area of 0.11 in.^{2}.

Table 3.1: Required area of transverse reinforcements compared to the prescribed area.

Spiral Type	Required Area in.^{2}	Prescribed Area in.^{2}	Spiral Size for Prescribed Area
Steel	—	0.034	W3.4
CFRP	0.018	0.024	0.2 Ø
GFRP	0.061	0.11	#3

3.2.3 Size of CFRP and GFRP Spiral Based on Equivalent Steel Spiral Shear Capacity

This approach involves determining the shear capacity of conventional steel spirals and finding an FRP bar size that produces a similar performance. In general, the formula for the total nominal shear capacity, V_n, is equal to the sum of the concrete shear capacity, V_c, and the transverse reinforcement shear capacity, V_s as shown in Equation (3.3).

$$V_n = V_c + V_s \tag{3.3}$$

This section focuses on the shear contribution from the spirals, that is, steel, CFRP and GFRP spirals. According to ACI 440.1R-15, the mechanism for the shear capacity for steel and FRP reinforcements are similar. Accordingly, the shear contribution from the three spiral types are summarized in Table 3.2. However, it should be noted that the shear contribution for CFRP and GFRP spirals were calculated using two methods which resulted in different results. The first method is based on tensile strength estimates, when the strain limit is 0.004 as described in Section 3.2.2, while the second method is based on the tensile strength of the FRP spiral bent portion. ACI 440.1R-15 recommends selecting the least value of the tensile strength calculated by these methods in obtaining the tensile strength of the FRP for shear design. From Table 3.2, the values obtained for #3 GFRP spirals is adequate because it exceeds those of the standard steel and CFRP spiral. Detailed calculations for V_c and V_s are provided in Appendix I.

For the design specimen PSG2 (flexural and axial test specimen), V_s is the least of the values shown in Table 3.2 for GFRP, therefore, the value of V_c and V_n are 73.44 kips and 89.91 kips, respectively. However, if the contribution of the transverse reinforcement to the nominal shear capacity is ignored (i.e., V_s = 0), then V_n for PCG2 is taken as 73.44 kips.

Table 3.2: Comparison of the shear capacity of transverse reinforcement

Spiral Type	Shear Contribution from spirals (V_s) kips	Spiral Size
Steel	13.71	W3.4
CFRP	12.18^{*}	0.2 Ø
	$24.60^{\dagger}$	
GFRP	16.47^{*}	#3
	$26.61^{\dagger}$	

*Spiral shear contribution based on tensile strength estimates when the strain limit is 0.004

†Spiral shear contribution based on the tensile strength of the bent portion of the FRP spiral.

3.3 Specification for GFRP Spirals

GFRP spirals for reinforcing in concrete piling shall meet the requirements in ASTM D7957. Table 3.3 shows the physical and mechanical property requirements for GFRP spirals. The geometric and mechanical properties for GFRP bars are as shown in Table 3.4.

Table 3.3: Physical and mechanical property requirements for GFRP spirals

Property	Test Method	Requirement
Fiber mass fraction	ASTM D2584 or ASTM D3171	≥ 70 %
Short-term moisture absorption	ASTM D570, subsection 7.4; 24 hours immersion at 122°F	≤ 0. 25 %
Long-term moisture absorption	ASTM D570, subsection 7.4; immersion to full saturation at 122°F	≤ 1.0 %
Glass transition temperature (T_g)	ASTM E1356	Midpoint temperature 212 °F
Degree of cure	≥ 95 %	ASTM E2160
Measured cross sectional area	ASTM D7205/D7205M, subsection 11.2.5.1	Table 3.4

Ultimate tensile strength (UTS)	ASTM D7205/D7205M	Table 3.4
Tensile modulus of elasticity	ASTM D7205/D7205M	≥ 6,500 ksi
Ultimate tensile strain	ASTM D7205/D7205M	≥ 1.1 %
Alkali resistance with load	ASTM D7705/D7705M, procedure A. 90 days test duration at 140 °F.	Tensile strength retention ≥ 80 % of UTS
Strength of bends	ASTM D7914/D7914M	≥ 60 % of the values in Table 3.4

Table 3.4: Geometric and mechanical properties requirement for GFRP bars

Bar Size Designation	Nominal Bar Diameter in.	Nominal Cross-Sectional Area in.^{2}	Measured Cross-Sectional Area in.^{2}		Minimum Guaranteed Tensile Load kips
			Minimum	Maximum	
2	0.250	0.049	0.046	0.085	6.1
3	0.375	0.11	0.104	0.161	13.2
4	0.500	0.20	0.185	0.263	21.6
5	0.625	0.31	0.288	0.388	29.1
6	0.750	0.44	0.415	0.539	40.9
7	0.875	0.60	0.565	0.713	54.1
8	1.000	0.79	0.738	0.913	66.8
9	1.128	1.00	0.934	1.137	82.0
10	1.270	1.27	1.154	1.385	98.2

3.4 Design Calculations for Testing Related Properties

3.4.1 Prestress Loss Calculations

PCI Design Handbook (2010) recommends simple equations for estimating the reduction of tensile stress in prestressing strands. This stress reduction or prestress loss is due to concrete shortening around the strands, relaxation of stress in strands and external factors that reduce the total initial force in strands before it is applied to concrete. For each strand in pile specimens with an initial stress of 34 kips, total prestress losses were estimated to amount to 14.8 %. The total prestress loss (TL) is a summation of losses due to elastic shortening (ES), creep of concrete (CR), shrinkage of concrete (SH) and relaxation of the strands (RE) as shown in Equation (3.4).

$$\mathrm{TL} = \mathrm{ES} + \mathrm{CR} + \mathrm{SH} + \mathrm{RE} \tag{3.4}$$

See Appendix E for detailed calculation of prestress losses.

3.4.2 Moment Capacity Calculations

Based on equilibrium equations using the rectangular stress block, the moment capacity of a pile specimen was calculated as shown in Appendix F. Strain compatibility assumptions were used by estimating the depth of the neutral axis, computing the strains in the strands, and determining the depth of the stress block. In addition, the forces in the concrete and in the strands were determined, and the sum of compression and tension forces were computed. For equilibrium, the neutral axis location was adjusted until the sum of compressive forces and tensile forces is equal to zero. The moment of these forces was then summed to obtain the nominal flexural strength of the pile specimen. From the calculations in Appendix F the nominal moment capacity at the pile section is 7524 kip-in.

3.4.3 Axial Capacity Calculations

According to PCI (1999), for a prestressed concrete compression member, the nominal axial load capacity is

$$\mathrm{P_o} = \left(0.85\mathrm{f'_c} - 0.6\mathrm{f_{pe}}\right)\mathrm{A_g} \tag{3.5}$$

PCI (1999, 2010) also provides service-load based allowable axial capacity, N, for prestressed concrete piles fully supported laterally by soil and primarily subjected to axial load as

$$\mathrm{N} = \left(0.33\mathrm{f'_c} - 0.27\mathrm{f_{pe}}\right)\mathrm{A_g} \tag{3.6}$$

As shown in Appendix G, $\mathrm{P_o}$ was calculated as 2582 kips while N was calculated as 981 kips. Note that $\mathrm{P_o}$ is relevant in the following discussions, whereas N is provided just as a reference.

Now, driving stress limits in compression were calculated using AASHTO (2017) and FDOT (2019) recommended equations. These equations are as follows:

$$\mathrm{S_{apc-AASHTO}} = \left(0.85\mathrm{f'_c} - \mathrm{f_{pe}}\right) \tag{3.7}$$

$$S_{apc-FDOT} = \left(0.7f'_c - 0.75f_{pe}\right) \tag{3.8}$$

Results in Appendix G show that the value of the driving stress limit in compression per AASHTO (2017) was 4.10 ksi, which is greater than the 3.45 ksi driving stress limit in compression calculated per FDOT (2019). Consequently, the forces corresponding to $S_{apc-AASHTO}$ and $S_{apc-FDOT}$ are 2351 kips and 1979 kips, respectively.

Also, the limits in tension were calculated using AASHTO (2017) and FDOT (2019) recommended equations. These equations are as follows:

$$S_{apt-AASHTO}\ \text{(normal environments)} = \left(0.095\sqrt{f'_c} + f_{pe}\right)\text{, in ksi} \tag{3.9}$$

$$S_{apt-AASHTO}\ \text{(corrosive environments)} = f_{pe} \tag{3.10}$$

$$S_{apt-FDOT}\ \text{(piles less than 50 ft.)} = \left(6.5\sqrt{f'_c} + 1.05f_{pce}\right)\text{, in psi} \tag{3.11}$$

AASHTO driving stress limits in tension for normal and corrosive environments were calculated as 1.24 ksi and 1.00 ksi, respectively. On the other hand, the FDOT driving stress limit in tension was calculated as 1.49 ksi. The detail of these calculations can be found in Appendix G.

3.4.4 Flexural Displacement Calculations

An 1,000 kip Enerpac actuator will be used to apply the flexural force to the pile (PSG2) using a spreader beam to generate the four point loading setup, which allows a consistent maximum moment over an extended length with no shear force, such that the beam will fail under pure bending (see Appendix A8) As shown in Appendix H, the actuator cracking load was calculated as approximately 33 kips and the load expected to fail the pile under flexure was predicted to be approximately 103 kips. The maximum displacement of the pile at midspan deflection due to the actuator load was calculated as 3.88 in. as shown in Appendix H. This theoretical deflection was calculated using the effective moment of inertia in Equation (*3.12*).

$$I_e = \left(\frac{M_{cr}}{M_a}\right)^3 I_g + \left[1 - \left(\left(\frac{M_{cr}}{M_a}\right)^3\right)\right] I_{cr}\ \text{(Article 5.6.3.5 of AASHTO (2017))} \tag{3.12}$$

3.4.5 Comparison of Results based on Design Concrete Properties and Expected As-built Concrete Properties

This section summarizes and compares design concrete property-based results and expected as-builts concrete property-based results for the calculations that were performed for testing related properties such as prestress losses, moment capacity, axial capacity, flexural displacement, and shear capacity. The following are the assumed concrete properties for design that were used in these calculations.

f'_{ci} = compressive strength in concrete at the time prestress is applied $= 4000$ psi

E_{ci} =modulus of elasticity of concrete at the time prestress is applied $= 57000\sqrt{f'_{ci}} = 3604996$ psi

f'_c = compressive strength in concrete at 28 days $= 6000$ psi

E_c = modulus of elasticity of concrete at 28 days $= 57000\sqrt{f'_c} = 4415201$ psi

However, for the expected as-built related results, the following concrete properties were used.

f'_{ci} = compressive strength in concrete at the time prestress is applied $= 5000$ psi (at 24 hours)

E_{ci} =modulus of elasticity of concrete at the time prestress is applied $= 57000\sqrt{f'_{ci}} = 4030508$ psi

f'_c = compressive strength in concrete at 28 days $= 9000$ psi

E_c = modulus of elasticity of concrete at 28 days $= 57000\sqrt{f'_c} = 5407494$ psi

The expected as-built related properties are approximated from the numbers reported by Roddenberry et al. (2014) (p. 146).

The comparison of results based on design concrete properties and expected as-built concrete properties are presented in Table 3.5.

Table 3.5: Comparison of results based on design vs. expected as-built concrete strength

Results	TL psi	f_{pe} ksi	M_n kip-in.	$S_{apc\text{-}FDOT}$ ksi	$S_{apt\text{-}FDOT}$ ksi	δ_{act} in.	V_c kips	V_n kips
Design	29960	1.00	7524	3.45	1.49	3.88	73.44	89.91
As built	26701	1.02	8361	5.55	1.61	3.91	87.38	101.09

TL = total prestress losses, f_{pe} = compressive stress in pile due to effective prestress, M_n = nominal moment capacity. $S_{apc\text{-}FDOT}$ = FDOT maximum allowable driving stress (compression stress limit), $S_{apt\text{-}FDOT}$ = FDOT maximum allowable driving stress (tension stress limit), δ_{act} = displacement due to actuator load, V_c = concrete contribution to nominal shear resistance, V_n = GFRP spiral contribution to nominal shear resistance.

Bibliography

AASHTO. (2012). *AASHTO LRFD Bridge Design Specification, 6th Ed*. American Association of State Highway and Transportation Officials, Washington, D.C.

AASHTO. (2017). *AASHTO LRFD Bridge Design Specification, 8th Ed*. American Association of State Highway and Transportation Officials, Washington, D.C.

AASHTO. (2018). *AASHTO Guide Specifications for the Design of Concrete Bridge Beams Prestressed with Carbon Fiber-Reinforced Polymer (CFRP) Systems, 1st Ed*. American Association of State Highway and Transportation Officials, Washington, D.C.

ACI. (2014). *ACI 318-14 Building Code Requirements for Structural Concrete*. American Concrete Institute Farmington Hills, MI.

ACI. (2015). *ACI 440.1 R-15 Guide for the Design and Construction of structural concrete reinforced with Fiber Reinforced Polymer (FRP) bars*. American Concrete Institute Farmington Hills, MI.

ASTM A1064-18a. (2018). *Standard Specification for Carbon-Steel Wire and Welded Wire Reinforcement, Plain and Deformed, for Concrete*. American Society for Testing and Materials, West Conshohocken, PA.

ASTM D4945-17. (2017). Standard Test Method for High-Strain Dynamic Testing of Deep Foundations. In *American Society for Testing and Materials*. American Society for Testing and Materials, West Conshohocken, PA.

ASTM D7957-17. (2017). Solid Round Glass Fiber Reinforced Polymer Bars for Concrete Reinforcement. In *American Society for Testing and Materials*. American Society for Testing and Materials, West Conshohocken, PA.

CSA-806. (2012). Design and construction of building components with fibre-reinforced polymers. In *CSA S806-12*.

FDOT. (2019). *FDOT Standard Specifications for Road and Bridge Construction*. Florida Department of Transportation, Tallahassee, FL.

Graybeal, B., & Pessiki, S. P. (1998). *Confinement Effectiveness of High Strength Spiral Reinforcement in Prestressed Concrete Piles*.

Hawkins, N. M., Kuchma, D. A., Mast, R. F., Marsh, M. L., & Reineck, K. (2005). *NCHRP Report 549: Simplified Shear Design of Structural Concrete Members*. Transportation Research Board, Washington, DC.

McVay, M., Bloomquist, D., Xie, Y., Johnson, J., Ko, J., Wasman, S., & Faraone, Z. (2009). Analyses of Embedded Data Collector (EDC). *Final Report, Department of Civil and Coastal Engineering University of Florida.*

PCI. (1999). *PCI Design Handbook: Precast and prestressed concrete, 6th Ed.* Precast/Prestressed Concrete Institute, Chicago, IL.

PCI. (2010). *PCI Design Handbook: Precast and Prestressed Concrete, 7th Ed.* Precast/ Prestressed Concrete Institute, Chicago, IL.

Roddenberry, M., Mtenga, P., & Joshi, K. (2014). Investigation of carbon fiber composite cables (CFCC) in prestressed concrete piles. *Final Rep., Florida Dept. of Transportation, Tallahassee, FL., BDK83-977–17*.

Appendices

Appendix A Instrumentation Plan

A1 Pile Information

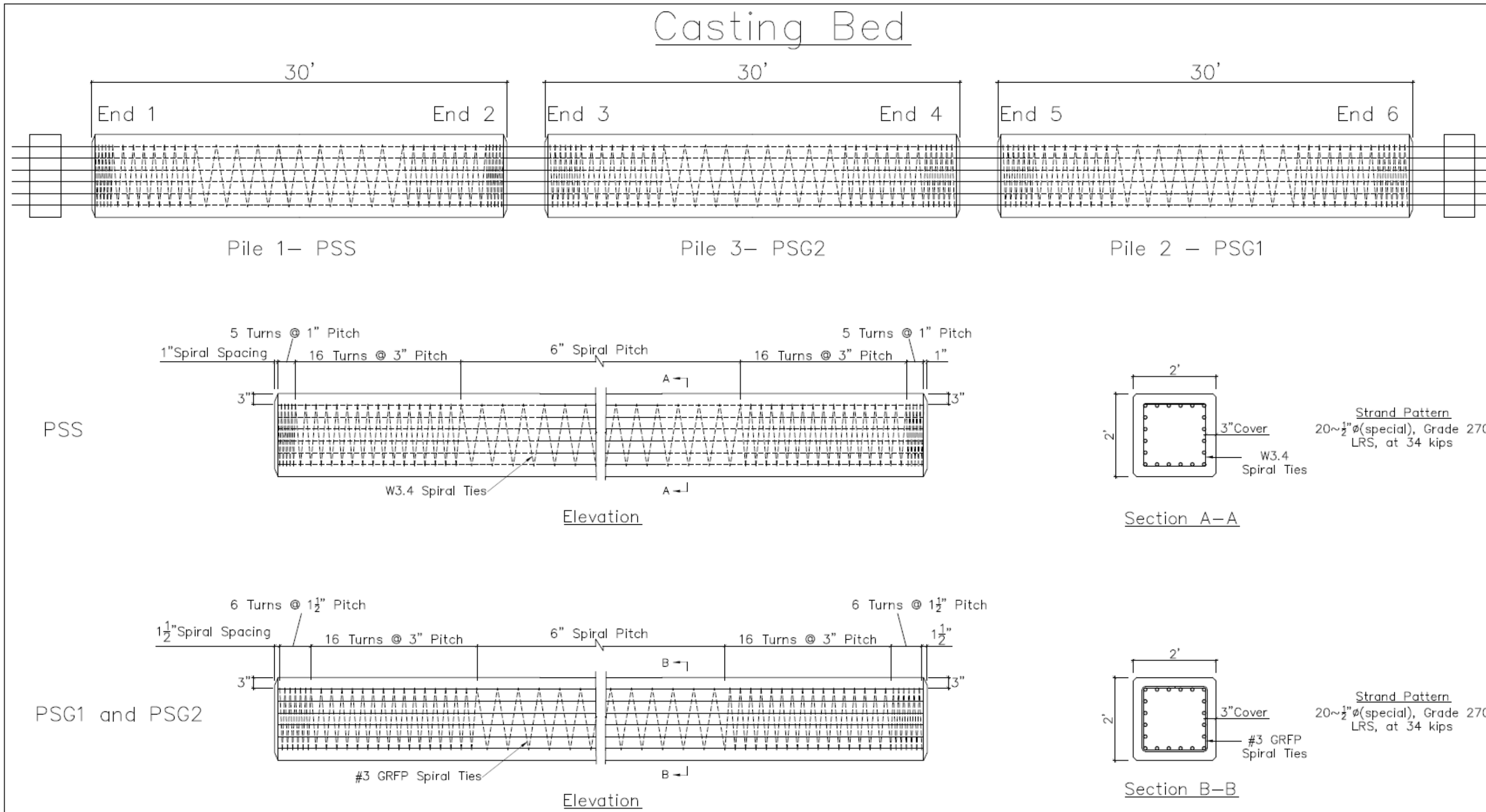

NOTES:

Pile nomenclature: The first letter 'P' represents 'pile'. The second letter represents the type of longitudinal reinforcement. The last letter represents the type of spiral used. For Example PSG is a pile with steel longitudinal reinforcement and GFRP spirals. 'S' is for prestressing steel and 'C' is for CFRP.

Concrete: Class V (special) according to FDOT Standard Plans specification.

Instrumentation Plan for Test Piles				Revisions:		
Pile Information	04/27/2020	FAMU-FSU College of Engineering	Sheet 1 of 16			

A2 Instrumentation Numbering

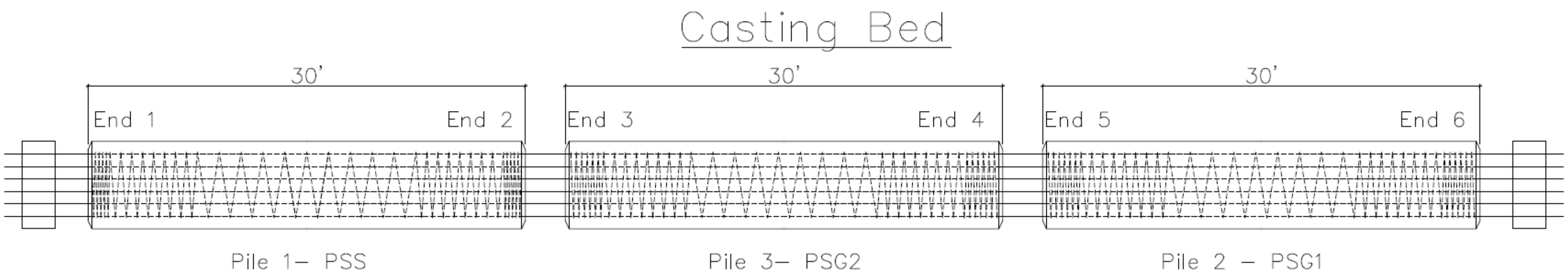

Pile Description	Internal Strain Gauges	Vibrating Wires	Fiber Optic Gauges
Pile1 – PSS	S1 – S52	–	FG1 & FG2
Pile2 – PSG1	S53 – S104	–	FG3 & FG4
Pile3 – PSG2	S105 – S132	VW1 – VW8	FG5 & FG6
Pile4 – PCC	–	–	–

Pile Description	External Strain Gauges	Deflection Gauges	EGCS–D5 Accelerometers	PDA Accelerometer/Strain Gauges	Break Beam Sensors and High Speed Cameras
Pile1 – PSS	–	–	✓	✓	✓
Pile2 – PSG1	–	–	✓	✓	✓
Pile3 – PSG2	SE1 – SE36	D1 – D12	–	–	–
Pile4 – PCC	–	–	✓	✓	✓

NOTES: 1. The table here–in shows the numbering for the vibrating wire strain gauges, fiber optic gauge strips, deflection gauges, and the internal and external foil strain gauges for the test piles.
2. Pile nomenclature: The first alphabet 'P' represents 'pile'. The second alphabet represents the type of longitudinal reinforcement. The last alphabet represents the type of spiral used. For Example PSG is a pile with steel longitudinal reinforcement and GFRP spirals. 'S' is for prestressing steel and 'C' is for CFRP.
3. See sheet 16 for PDA instrumentation.

Instrumentation Plan for Test Piles				Revisions:		
Instrumentation Numbering	04/27/2020	FAMU-FSU College of Engineering	Sheet 2 of 16			

A3 Tests and Sensors Monitored

Tests and Sensors Being Monitored

For the tests number 1 to 4, the gauges are accompanied by green circles while the inactive gauges are accompanied by red circles.

1. Strand Detensioning: Fiber optic gauges in PSS, PSG1 and PSG2 will be monitored during the detensioning process.

Pile Description	Internal Strain Gauges	Vibrating Wires	Fiber Optic Gauges
Pile1 – PSS	S1 – S52 🔴	–	FG1 & FG2 🟢
Pile2 – PSG1	S53 – S104 🔴	–	FG3 & FG4 🟢
Pile3 – PSG2	S105 – S132 🔴	VW1 – VW8 🔴	FG5 & FG6 🟢
Pile4 – PCC	–	–	–

Pile Description	External Strain Gauges	Deflection Gauges	EGCS–D5 Accelerometers	PDA Accelerometer/Strain Gauges	Break Beam Sensors and High Speed Cameras
Pile1 – PSS	–	–	✓ 🔴	✓ 🔴	✓ 🔴
Pile2 – PSG1	–	–	✓ 🔴	✓ 🔴	✓ 🔴
Pile3 – PSG2	SE1 – SE36 🔴	D1 – D12 🔴	–	–	–
Pile4 – PCC	–	–	✓ 🔴	✓ 🔴	✓ 🔴

Instrumentation Plan for Test Piles				Revisions:
Tests and Sensors Monitored	04/27/2020	FAMU-FSU College of Engineering	Sheet 3 of 16	

Tests and Sensors Being Monitored

For the tests number 1 to 4, the gauges are accompanied by green circles while the inactive gauges are accompanied by red circles.

2. Impact Tests: Specimens PSS, PSG1 and PCC will be subjected to impact tests. In addition to the active gauges indicated, the accelerometer mounted on the impactor and PDA instrumentation on the piles will be monitored.

Pile Description	Internal Strain Gauges	Vibrating Wires	Fiber Optic Gauges
Pile1 – PSS	S1 – S52 🟢	–	FG1 & FG2 🔴
Pile2 – PSG1	S53 – S104 🟢	–	FG3 & FG4 🔴
Pile3 – PSG2	S105 – S132 🔴	VW1 – VW8 🔴	FG5 & FG6 🔴
Pile4 – PCC	–	–	–

Pile Description	External Strain Gauges	Deflection Gauges	EGCS–D5 Accelerometers	PDA Accelerometer/Strain Gauges	Break Beam Sensors and High Speed Cameras
Pile1 – PSS	–	–	✓ 🟢	✓ 🟢	✓ 🟢
Pile2 – PSG1	–	–	✓ 🟢	✓ 🟢	✓ 🟢
Pile3 – PSG2	SE1 – SE36 🔴	D1 – D12 🔴	–	–	–
Pile4 – PCC	–	–	✓ 🟢	✓ 🟢	✓ 🟢

Instrumentation Plan for Test Piles				Revisions:
Tests and Sensors Monitored	04/27/2020	FAMU-FSU College of Engineering	Sheet 4 of 16	

Tests and Sensors Being Monitored

For the tests number 1 to 4, the gauges are accompanied by green circles while the inactive gauges are accompanied by red circles.

3. Flexural Test: Specimen PSG2 will be tested under flexure.

Pile Description	Internal Strain Gauges	Vibrating Wires	Fiber Optic Gauges
Pile1 – PSS	S1 – S52 🔴	–	FG1 & FG2 🔴
Pile2 – PSG1	S53 – S104 🔴	–	FG3 & FG4 🔴
Pile3 – PSG2	S105 – S132 🔴	VW1 – VW8 🔴	FG5 & FG6 🔴
Pile4 – PCC	–	–	–

Pile Description	External Strain Gauges	Deflection Gauges	EGCS–D5 Accelerometers	PDA Accelerometer/Strain Gauges	Break Beam Sensors and High Speed Cameras
Pile1 – PSS	–	–	✓ 🔴	✓ 🔴	✓ 🔴
Pile2 – PSG1	–	–	✓ 🔴	✓ 🔴	✓ 🔴
Pile3 – PSG2	SE1 – SE36 🟢	D1 – D12 🟢	–	–	–
Pile4 – PCC	–	–	✓ 🔴	✓ 🔴	✓ 🔴

Instrumentation Plan for Test Piles				Revisions:
Tests and Sensors Monitored	04/27/2020	FAMU-FSU College of Engineering	Sheet 5 of 16	

Tests and Sensors Being Monitored

For the tests number 1 to 4, the gauges are accompanied by green circles while the inactive gauges are accompanied by red circles.

4. Axial Test: Part of specimen PSG2 will be utilized for the axial test.

Pile Description	Internal Strain Gauges	Vibrating Wires	Fiber Optic Gauges
Pile1 – PSS	S1 – S52 ●	–	FG1 & FG2 ●
Pile2 – PSG1	S53 – S104 ●	–	FG3 & FG4 ●
Pile3 – PSG2	S105 – S132 ●	VW1 – VW8 ●	FG5 & FG6 ●
Pile4 – PCC	–	–	–

Pile Description	External Strain Gauges	Deflection Gauges	EGCS–D5 Accelerometers	PDA Accelerometer/Strain Gauges	Break Beam Sensors and High Speed Cameras
Pile1 – PSS	–	–	✓ ●	✓ ●	✓ ●
Pile2 – PSG1	–	–	✓ ●	✓ ●	✓ ●
Pile3 – PSG2	SE1 – SE36 ●	D1 – D12 ●	–	–	–
Pile4 – PCC	–	–	✓ ●	✓ ●	✓ ●

Instrumentation Plan for Test Piles				Revisions:
Tests and Sensors Monitored	04/27/2020	FAMU-FSU College of Engineering	Sheet 6 of 16	

A4 Internal (Spiral) Strain Gauge and Fiber Optic Gauge Instrumentation for PSS

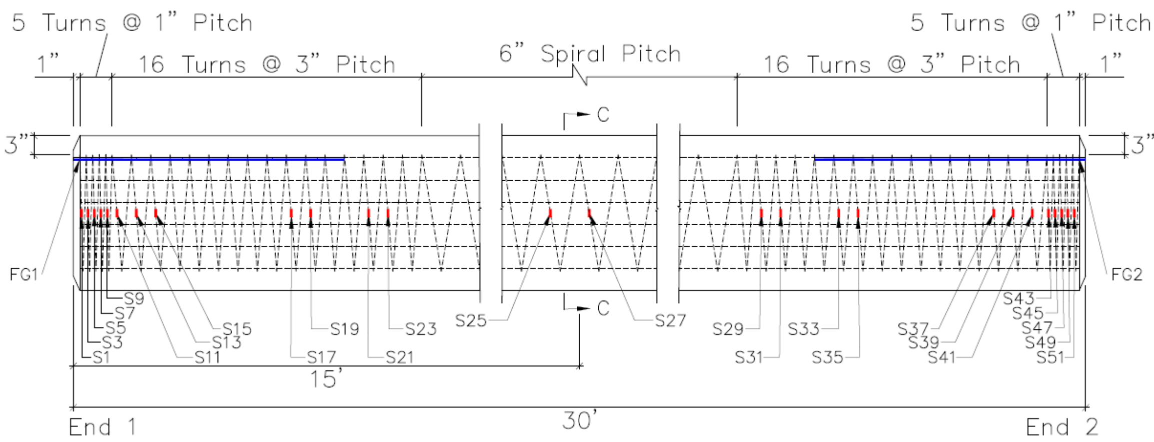

PSS – East View

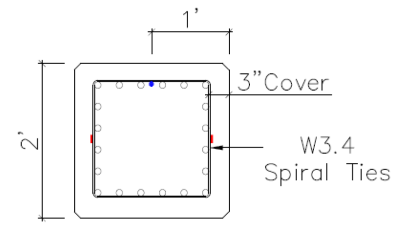

Section C–C

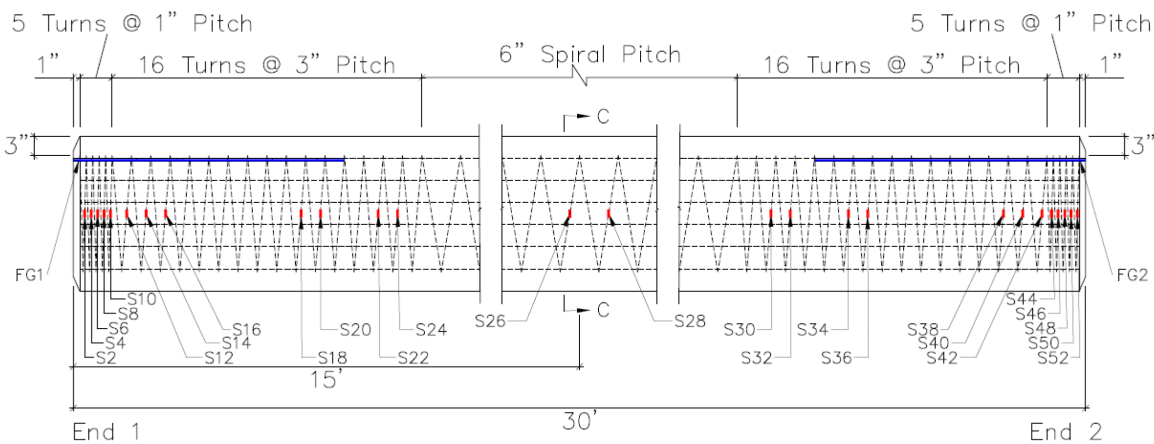

PSS – West View

NOTES:

1. PSS is longitudinally reinforced by 20 strands ~ $\frac{1}{2}$"ø(special), Grade 270 Low–lax steel and transversely by W3.4 steel spirals
2. S# represents foil strain gauges attached to the spirals.
3. The 5 mm foil strain gauges are represented by red rectangles.
4. Gauge installation is from left to right.
5. The foil strain gauges will be attached to spirals on opposite sides of the pile along the center of the pile.
6. Gauges are attached longitudinally on the spirals.
7. Gauges are attached on opposite sides of the first 8 spiral turns from both ends of the pile.
8. Gauges are attached to spirals on opposite sides of the pile around the 3ft. and 4ft. mark (or 1.5 and 2 x pile width) from both ends of the pile.
9. Also spirals on both sides of the pile center (15ft. from the ends) will be instrumented with gauges on either sides of the pile.
10. The strain gauges are monitored during the impact test.
11. FG# represents 42" long fiber optic gauges placed at both ends of the pile.
12. The FG# gauges are monitored when detensioning the strands.

Instrumentation Plan for Test Piles				Revisions:		
Internal (Spiral) Strain Gauges and Fiber Optic Gauges	04/27/2020	FAMU-FSU College of Engineering	Sheet 7 of 16			

A5 Internal (Spiral) Strain Gauge and Fiber Optic Gauge Instrumentation for PSG1

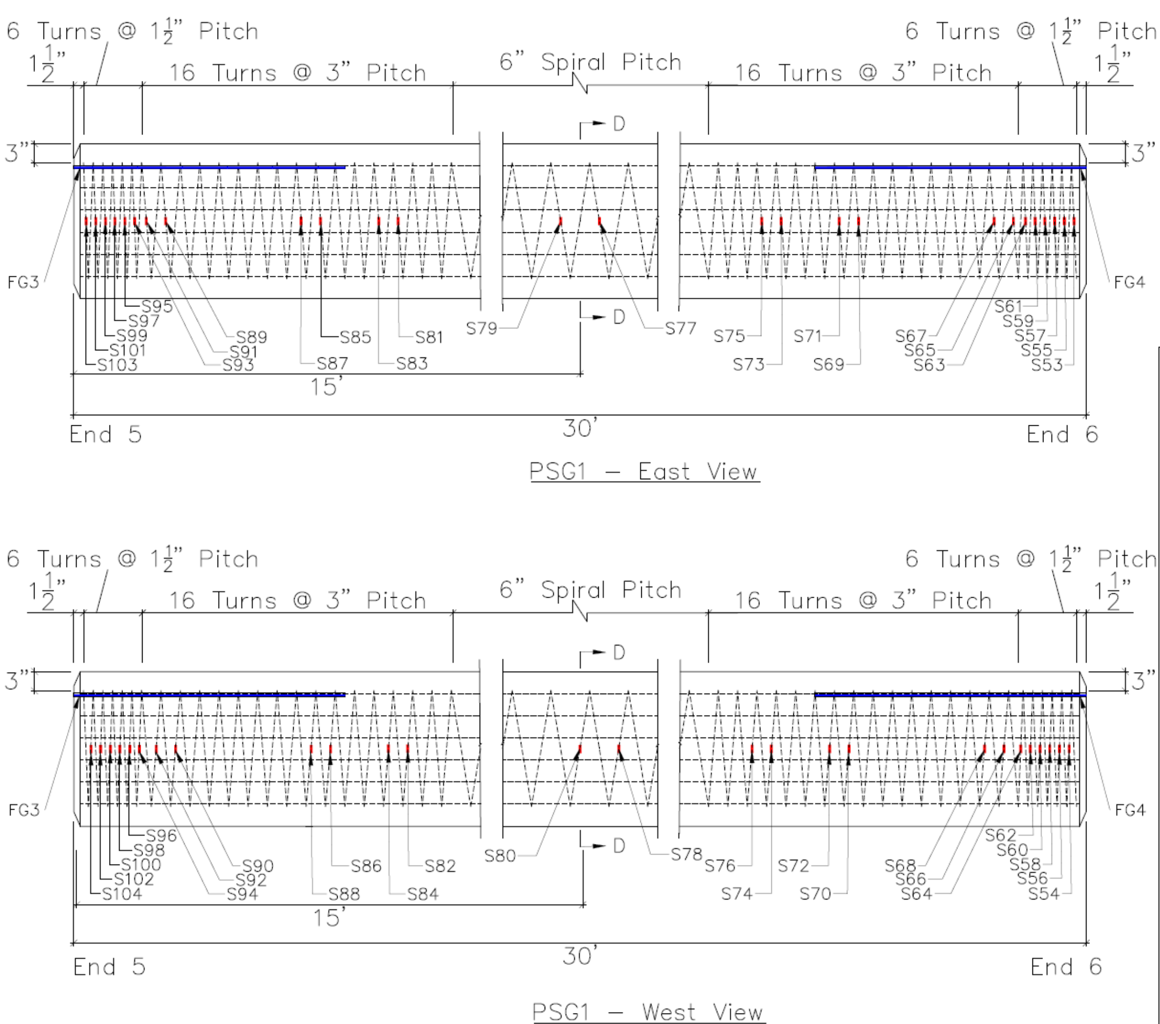

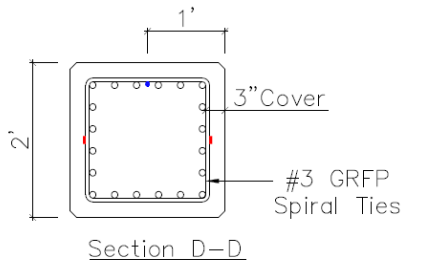

NOTES:

1. PSG1 is longitudinally reinforced by 20 strands ~ ½"ø(special), Grade 270 Low–lax steel and transversely by #3 GFRP spirals.
2. Gauge numbering is from right to left to match PSS1(End 1) with PSG1(End 6).
3. S# represents foil strain gauges attached to the spirals.
4. The 5 mm foil strain gauges are represented by red rectangles.
5. The foil strain gauges will be attached to spirals on opposite sides of the pile along the center of the pile.
6. Gauges are attached longitudinally on the spirals.
7. Gauges are attached on opposite sides of the first 8 spiral turns from both ends of the pile.
8. Gauges are attached to spirals on opposite sides of the pile around the 3ft.and 4ft. mark (or 1.5 and 2 x pile width) from both ends of the pile.
9. Also spirals on both sides of the pile center (15ft. from the ends) will be instrumented with gauges on either sides of the pile.
10. The strain gauges are monitored during the impact test.
11. FG# represents 42" long fiber optic gauges placed at both ends of the pile.
12. The FG# gauges are monitored when detensioning the strands.

Instrumentation Plan for Test Piles				Revisions:		
Internal (Spiral) Strain Gauges and Fiber Optic Gauges	04/27/2020	FAMU-FSU College of Engineering	Sheet 8 of 16			

A6 Internal (Spiral) Strain Gauge, Fiber Optic Gauge and Vibrating Wire Instrumentation for PSG2

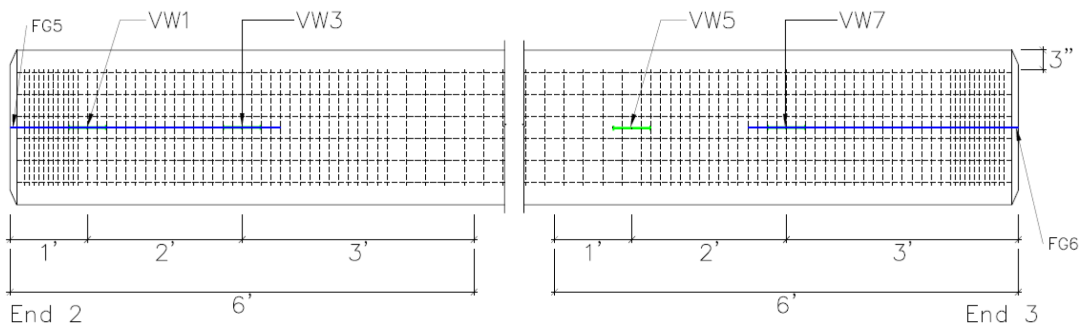

PSG2 Top View

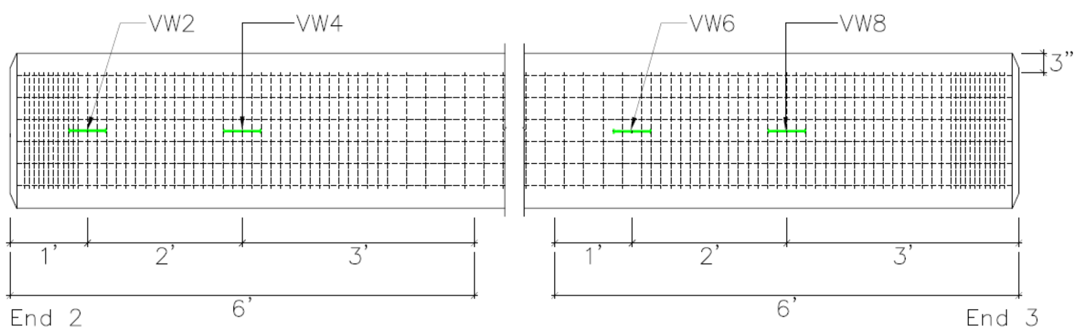

PSG2 Bottom View

NOTES:

1. Same reinforcement as PSG1.
2. VW# represents vibrating wire strain gauges.
3. The Geokon – 4200 vibrating wire is represented by green rectangles.
4. S# represents foil strain gauges attached to the spirals longitudinally.
4. Gauge installation is from right to left.
5. The 5 mm foil strain gauges are represented by red rectangles.
6. Instrumentation to the left of the drawing (End 2) is such that gauges are closer to the end of the pile.
7. Instrumentation to the right of the drawing is such that gauges are closer to the pile cut–off point.
8. Vibrating wires are embedded within the top and bottom facing sides of the pile.
9. Strain gauges are embedded within the east and west facing sides of the pile.
10. Install VW gauges within the concrete core in the longitudinal direction. VWs are offset from the spirals as shown on sheet 10 and 11.
11. Ensure VW gauges are firmly tied before concrete is poured.
12. Vibrating wire cables shall be numbered and passed to the top surface of the pile.
13. The pile will be cut 6ft. from both ends for axial testing after flexural tests have been concluded.
14. See Sheet 15 for cable routing.
15. These gauges are monitored during the axial test.
16. FG# represents 42" long fiber optic gauges placed at both ends of the pile.
17. The FG# gauges in PSG2 are monitored when detensioning the strands and during the axial test.

Instrumentation Plan for Test Piles				Revisions:		
Vibrating Wires, Strain Gauges and Fiber Optics for Axial Test	04/27/2020	FAMU-FSU College of Engineering	Sheet 9 of 16			

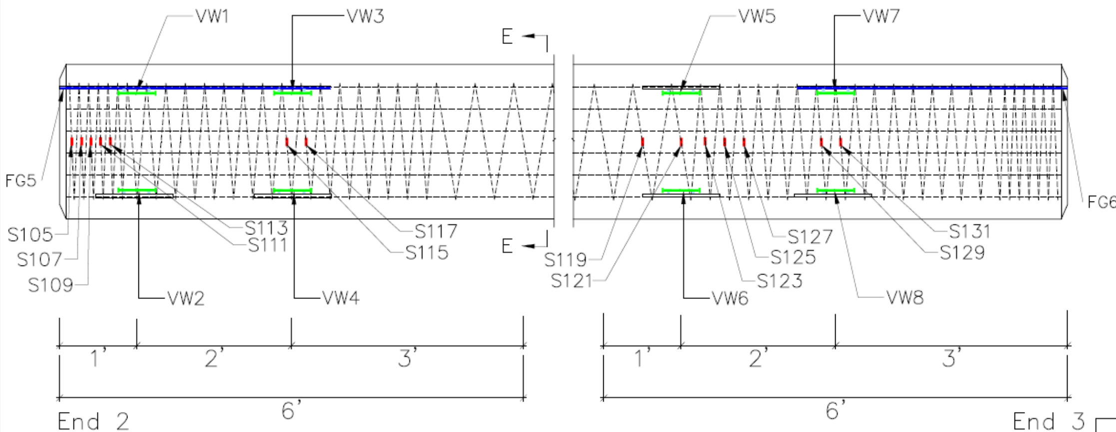

PSG2 East View

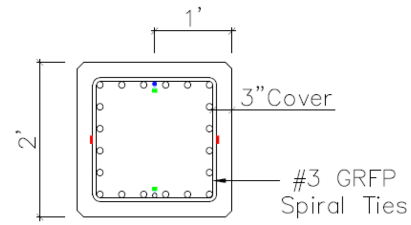

Section E–E

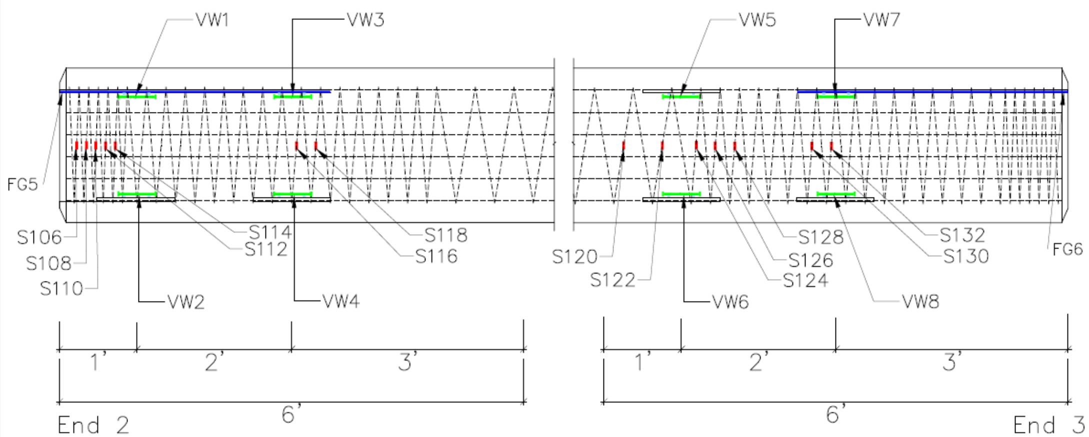

PSG2 West View

NOTE:

Same as previous sheet

Instrumentation Plan for Test Piles				Revisions:		
Vibrating Wires and Strain Gauges for Axial Test	04/27/2020	FAMU-FSU College of Engineering	Sheet 10 of 16			

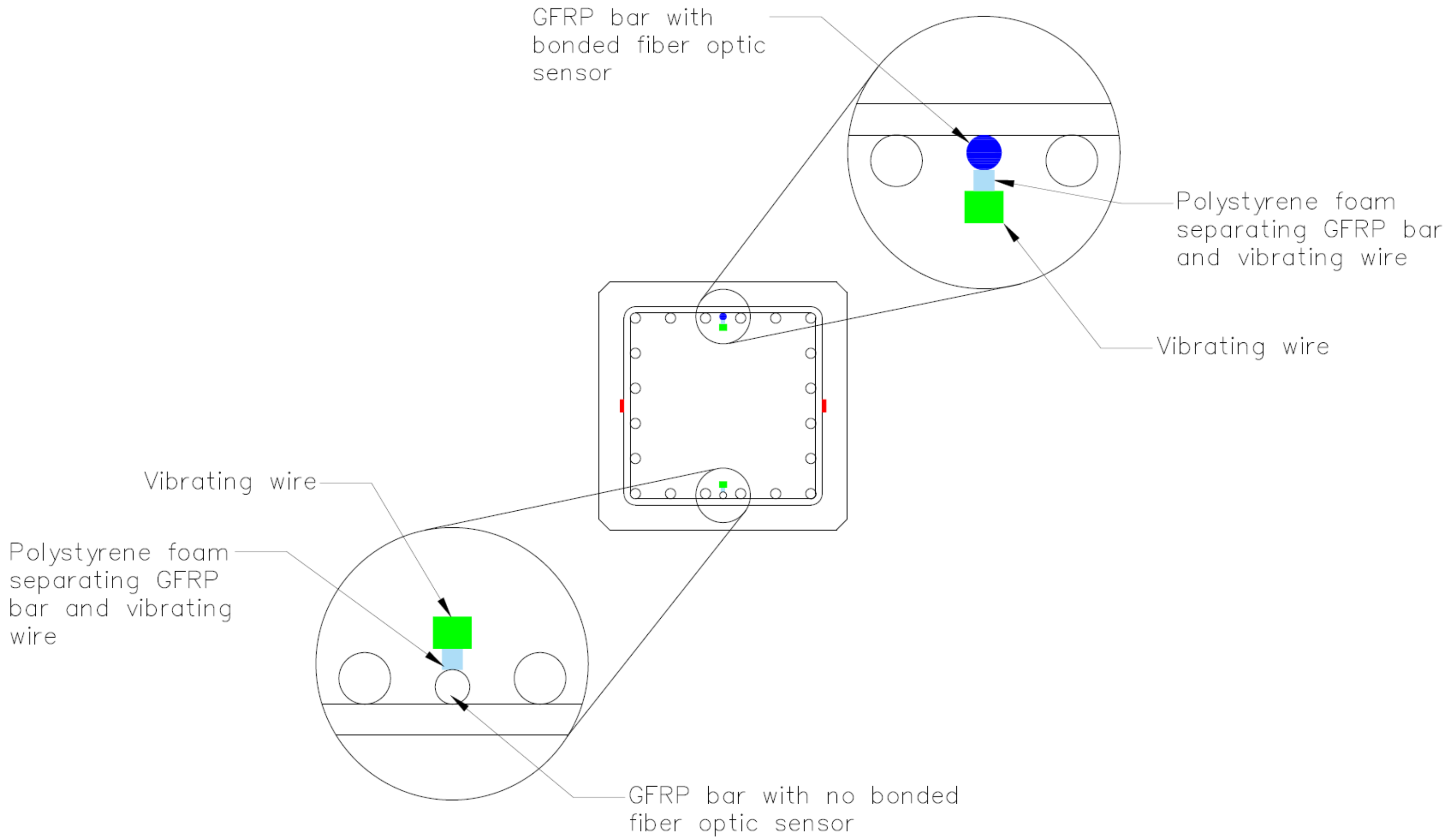

Instrumentation Plan for Test Piles				Revisions:		
Gauge Details PSG2	04/27/2020	FAMU-FSU College of Engineering	Sheet 11 of 16			

A7 Axial Test Setup

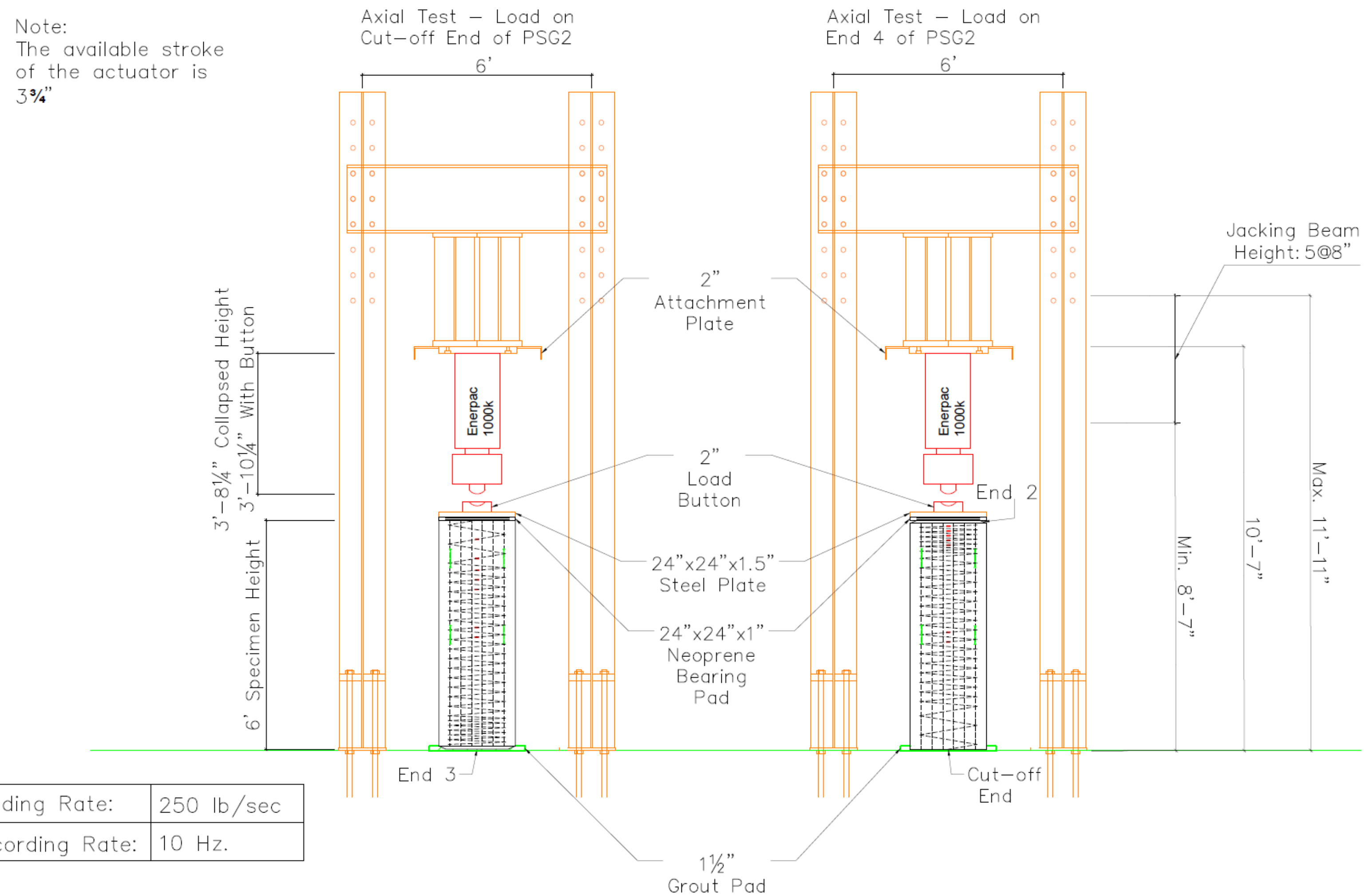

Loading Rate:	250 lb/sec
Recording Rate:	10 Hz.

Instrumentation Plan for Test Piles				Revisions:		
Axial Test Setup	04/27/2020	FAMU-FSU College of Engineering	Sheet 12 of 16			

A8 Flexural Test Setup/Instrumentation

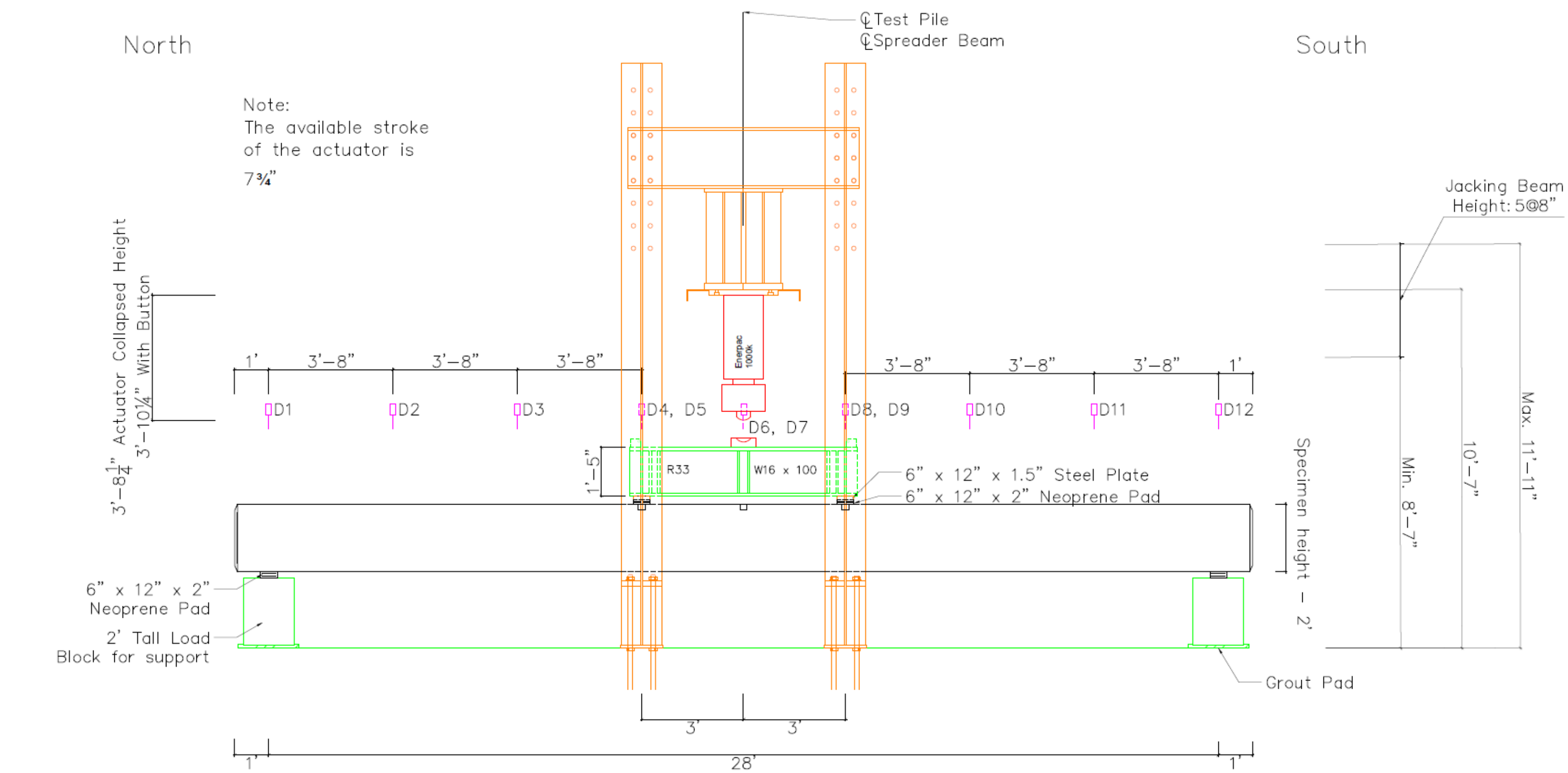

NOTE:

1. D# represents laser deflection gauges. Dimension shown are center to center of deflection gauges.
2. SE# represent 60 mm external strain gauges. Dimension shown on Sheet 14 are center to center of strain gages.
3. As shown on sheet 14 gauges D4, D5, D6, D7, D8 and D9 need 2 in. angles glued to the top side of the specimen to avoid interference with the spreader beam.

Load Rate:	250 lb/sec, then 200 lb/sec after the first flexural crack
Recording Rate:	10 Hz.
Predicted Load at Cracking :	33 kips (due to actuator)
Predicted Load at Flexural Failure:	103 kips
Predicted Deflection:	3.88 in.(when the actuator load=103 kips)

Instrumentation Plan for Test Piles				Revisions:		
Flexural Test Instrumentation	04/27/2020	FAMU-FSU College of Engineering	Sheet 13 of 16			

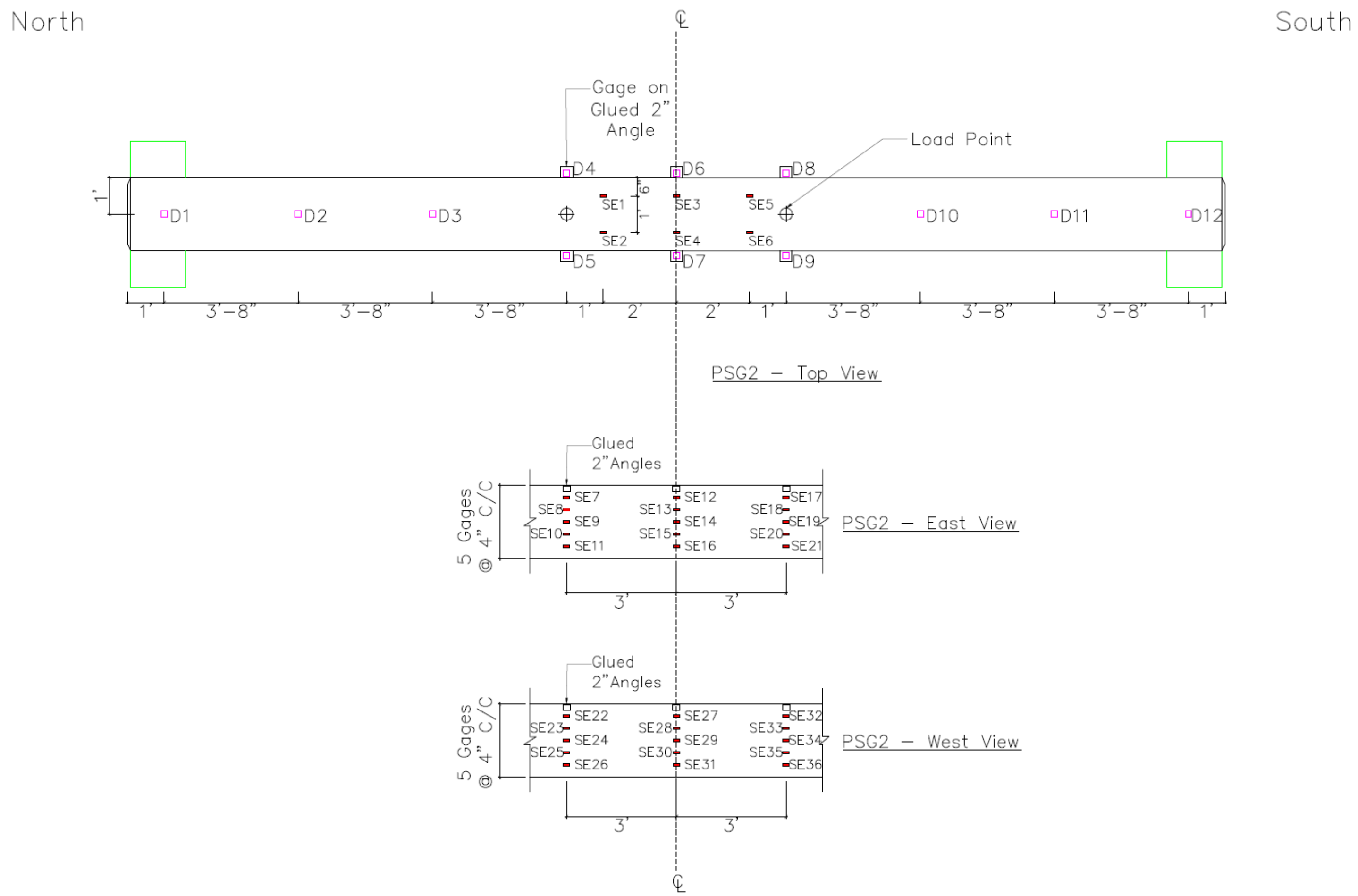

Instrumentation Plan for Test Piles				Revisions:		
Flexural Test Instrumentation	04/27/2020	FAMU-FSU College of Engineering	Sheet 14 of 16			

A9 Cable Routing for Internal Instrumentation

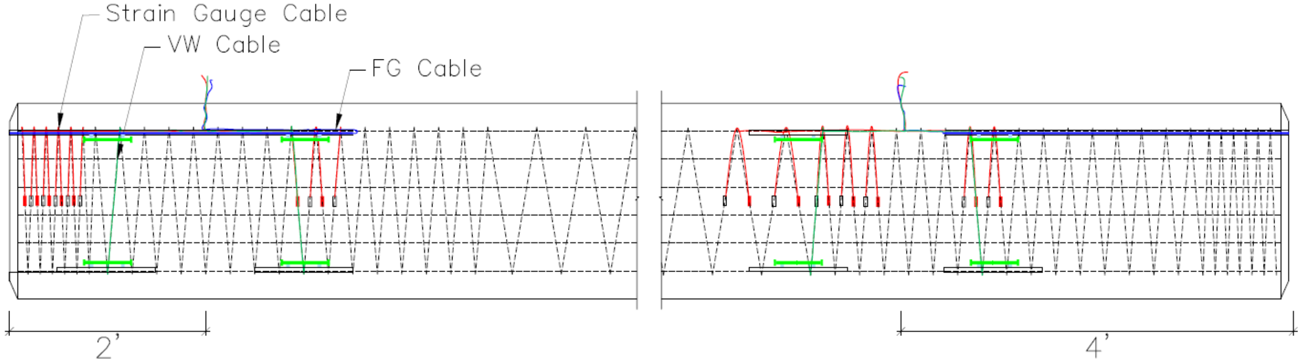

Internal Cable Routing (PSG2)

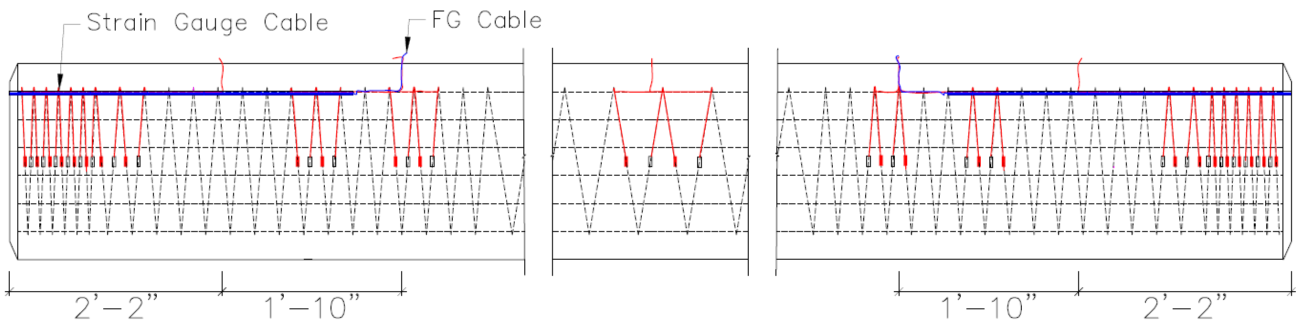

Internal Cable Routing (PSG1)

NOTE:
1. Cable routing for PSS follows a similar pattern to PSG1.
2. Red lines represent strain gauge cables.
3. Green lines represent vibrating wire cables.
4. Blue lines represent fiber optic gauge cables.

Instrumentation Plan for Test Piles				Revisions:		
Cable Routing	04/27/2020	FAMU-FSU College of Engineering	Sheet 15 of 16			

A10 PDA Instrumentation

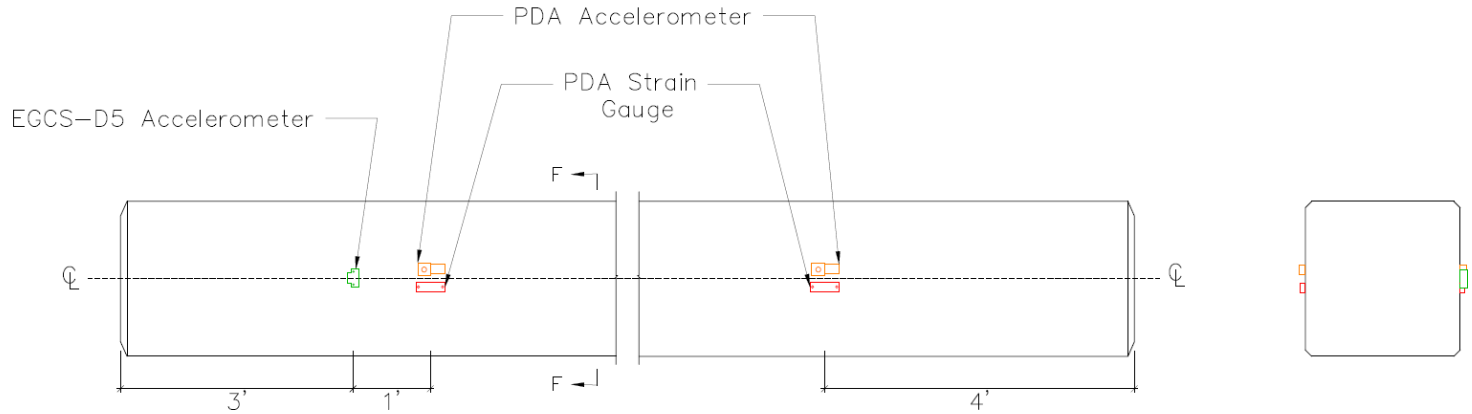

Section F–F

Side View and Cross Section of Instrumented Pile Showing the Layout of PDA Sensors and EGCS–D5 Accelerometer

NOTE:

1. PDA instrumentation is applicable to PSS, PSG1 and PCC.
2. EGCS–D5 is an accelerometer provided by the project team in order to obtain additional measurement at another point on the pile.

Instrumentation Plan for Test Piles				Revisions:		
PDA Instrumentation	04/27/2020	FAMU-FSU College of Engineering	Sheet 16 of 16			

Appendix B Data Sheet for EGCS-D5 Accelerometer

MODEL EGCS-D5 ACCELEROMETER

SPECIFICATIONS

- **Rugged Piezoresistive Design**
- **DC Response, Critically Damped**
- **±50g to ±10,000g Range**
- **DC to 10kHz Response**
- **Fits Popular Shock Accelerometer Mounting Bolt Pattern**

The Model EGCS-D5 accelerometer is critically damped with built-in over-range stops that are set to protect the unit against up to 20,000g shocks. This is ideal for applications which may experience rough handling or in situations where the accelerometer must survive a high initial overload in order to make a low g measurement. These units feature a Wheatstone Bridge output with compensated temperature range of +20 to +80ºC. An inline amplifier option is available for superior signal to noise performance.

dimensions

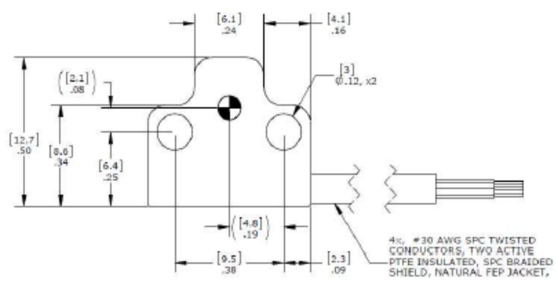

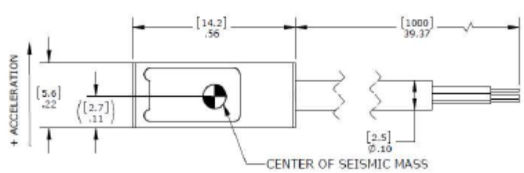

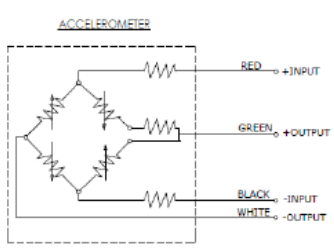

FEATURES

- **±50g to ±10,000g Dynamic Range**
- **Heavy Duty, Rugged**
- **Static and Dynamic Measurement**
- **DC to 10,000Hz Frequency Response**
- **±1% Non-Linearity**
- **-40ºC to +100ºC Temperature Range**
- **Inline Amplifier Option**

APPLICATIONS

- **Metal-to-Metal Mechanical Shock**
- **Impact Testing**
- **Building Construction**
- **Pile Driving**
- **Weapons Testing**

PERFORMANCE SPECIFICATIONS

All values are typical at +24°C, 80Hz and 15Vdc excitation unless otherwise stated. Measurement Specialties reserves the right to update and change these specifications without notice.

Parameters									
DYNAMIC									Notes
Range (g)	±50	±100	±250	±500	±1000	±2500	±5000	±10000	
Sensitivity (mV/g)[1]	4	2	0.8	0.4	0.2	0.08	0.04	0.016	
Frequency Response (Hz)	0-360	0-540	0-780	0-1050	0-1500	0-2100	0-2400	0-5000	+3%/-8%
Frequency Response (Hz)	0-600	0-900	0-1300	0-1750	0-2500	0-3500	0-4000	0-10000	+3%/-18%
Natural Frequency (Hz)	1200	1800	2600	3500	5000	7000	8000	16000	
Non-Linearity (%FSO)	±1	±1	±1	±1	±1	±1	±1	±1	
Transverse Sensitivity (%)	<3	<3	<3	<3	<3	<3	<3	<3	
Damping Ratio	0.7	0.7	0.7	0.7	0.7	0.7	0.7	0.7	Nominal
Shock Limit (g)	5000	10000	10000	10000	10000	10000	20000	20000	

ELECTRICAL	
Zero Acceleration Output (mV)	±20 Differential
Excitation Voltage (Vdc)	15 (can be used from 2 to 15Vdc but lower excitation voltage will decrease sensitivity accordingly)
Input Resistance (Ω)	2000 Nominal
Output Resistance (Ω)	1000 Nominal
Insulation Resistance (MΩ)	>100 @50Vdc
Ground Isolation	Isolated from Mounting Surface
ENVIRONMENTAL	
Thermal Zero Shift	±2.0mV / 50°C (±2.0mV / 100°F)
Thermal Sensitivity Shift	±2.5% / 50°C (±2.5% / 100°F)
Operating Temperature	-40 to +100°C (-40 to +212°F)
Compensated Temperature	+20 to+80°C (+70 to +170°F), contact factory for other temperature compensation options
Storage Temperature	-40 to +100°C (-40 to +212°F)
Humidity	Epoxy Sealed, IP65
PHYSICAL	
Case Material	Stainless Steel
Cable	4x #30 AWG Leads, PTFE Insulated, Braided Shield, FEP Jacket
Weight	8 grams
Mounting	Screw Mount, 2x #4-40 Socket Head Cap Screws

[1] Output is ratiometric to excitation voltage

Calibration supplied:	CS-FREQ-0100	NIST Traceable Amplitude Calibration from 20Hz to Frequency Response Limit
Optional accessories:	AC-D05201	Triaxial Mounting Block
	121	3-Channel Precision Low Noise DC Amplifier
	140A	Auto-zero Inline Amplifier
	145	Dedicated Inline Amplifier (see next page)

Optional 145 Inline Amplifier Module

MODEL EGCS-D5 ACCELEROMETER

Unit with model 145 Inline Amplifier can be powered with 8-20Vdc. The sensor is supplied with regulated 5Vdc from the amplifier. The output is differential with a 2.5Vdc common mode. The amplifier has a 30x gain and a 20kHz low-pass filter and is intended for high-g ranges.

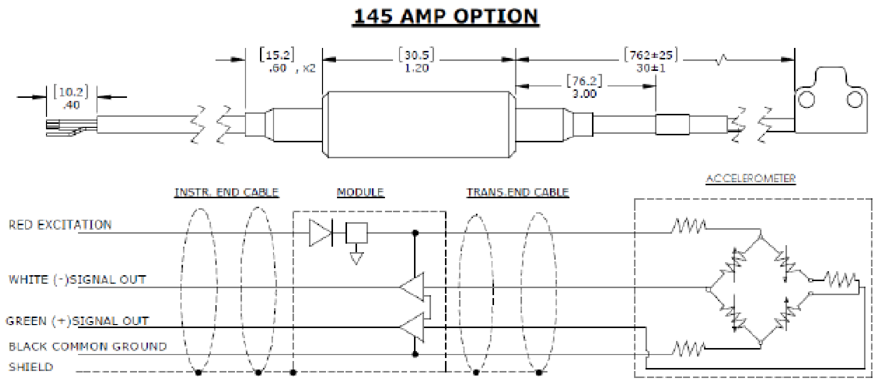

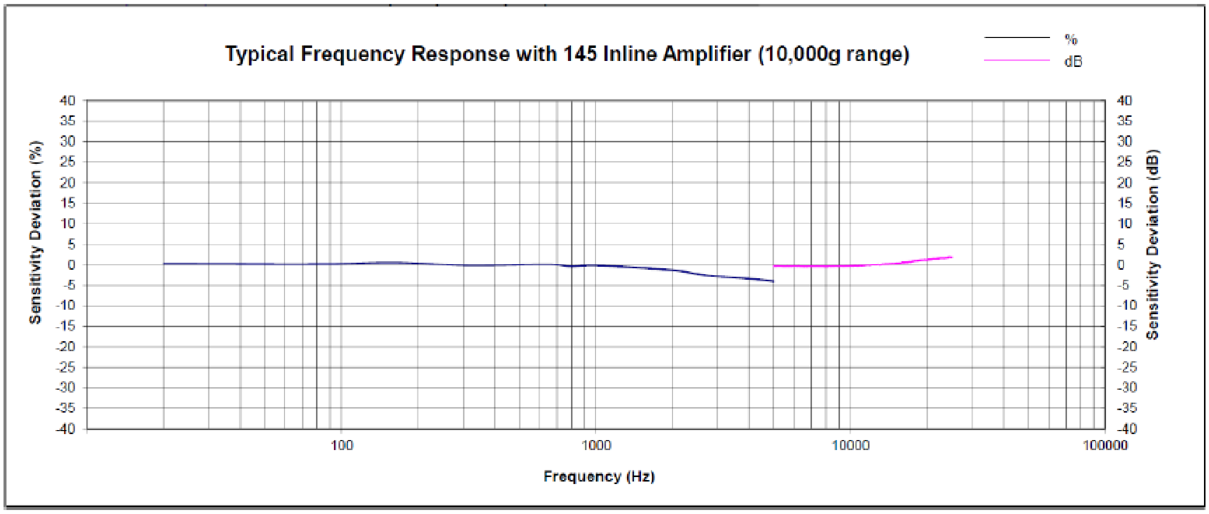

ORDERING INFO

```
EGCS–D5L–100–/Z1/L2M/145
            I    I        I___Options, otherwise leave blank
            I    I_________Range (100 is 100g)
            I______________Sensitive axis rotated 90°, otherwise blank
```

Compensated Temp Ranges:	Standard	=	+20 to +80°C +(70 to +170°F)
	Z*	=	Non standard, contact factory
Excitation Voltage:	Standard	=	15Vdc
	V*	=	Non standard, contact factory
Special Cable Length:	L00F	=	Replace "00" with length in feet
	L00M	=	Replace "00" with length in meter
Standard Unit with 145 Amplifier:	145	=	Inline amplifier added

Example: EGCS-D5-10000-/L2M
Model EGCS-D5, 10,000g Range, 2 Meter Cable Length

NORTH AMERICA
Measurement Specialties, Inc.,
a TE Connectivity Company
Phone: 800-522-6752
Email: customercare.hmpt@te.com

EUROPE
MEAS Deutschland GmbH(Europe)
a TE Connectivity Company
Phone: 800-440-5100
Email: customercare.lcsb@te.com

ASIA
Measurement Specialties (China), Ltd.,
a TE Connectivity Company
Phone: 0400-820-6015
Email: customercare.shzn@te.com

Appendix C Impact Test Setup

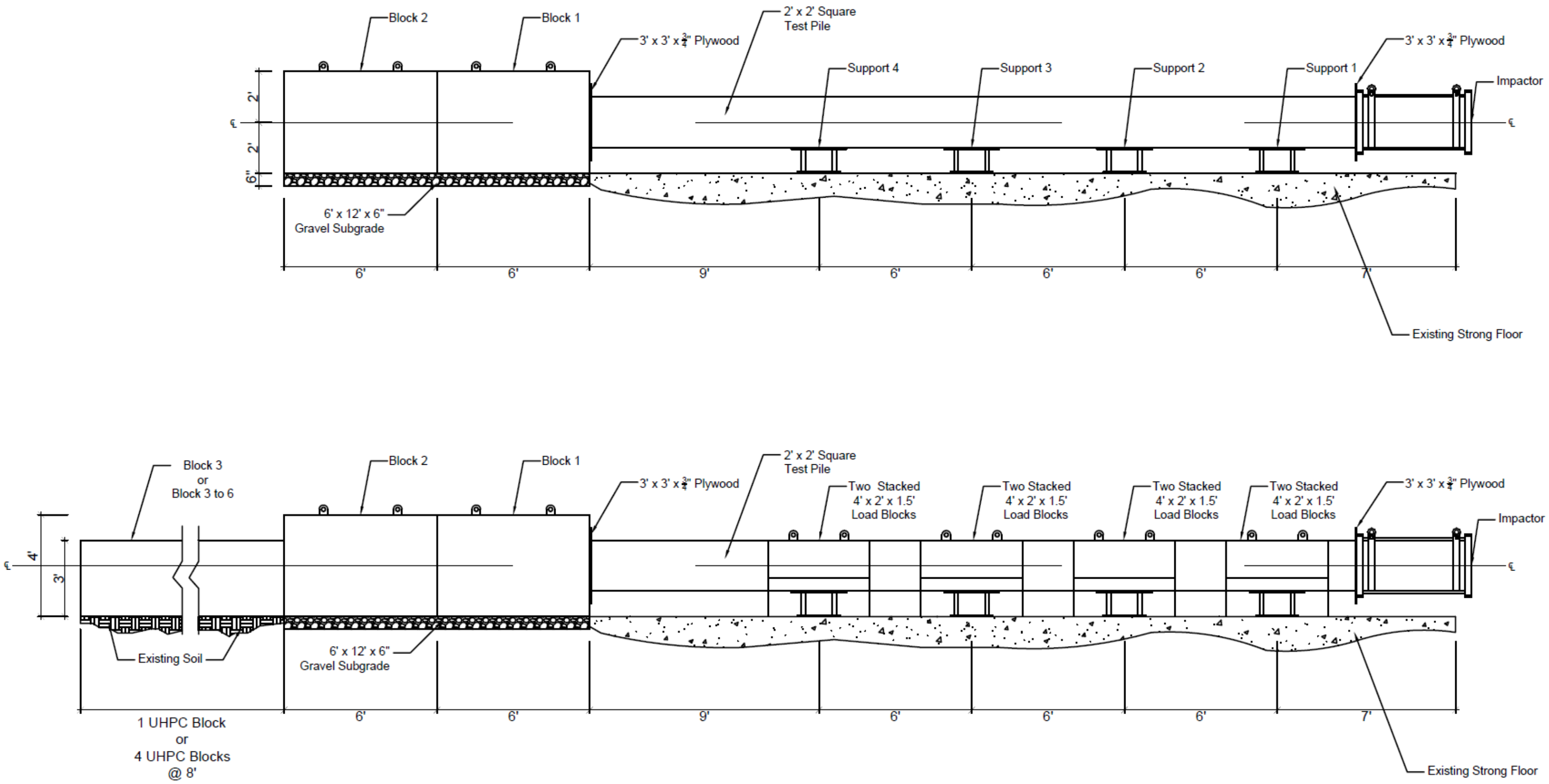

Impact Test Set-up Elevation

NOTE:
Extra restraint blocks placed behind blocks 1 and 2 as shown above.
FDOT load blocks placed for lateral support on either side of the pile supports.

Impact Test Set-up				Revisions:		
Impact Test Set-up Elevation	2019-05-24	FAMU-FSU College of Engineering	Sheet 27 of 27			

Appendix D Size of CFRP and GFRP Spiral Based on Force Equilibrium

The approach in this section assumes that the strength reduction because of spalling should be equal to the strength gain of the concrete core resulting from confinement. The following information was used for the calculations:

Compressive strength of concrete, $f'_c = 6$ ksi

Gross area, $A_g = 574\ \text{in}^2$

Concrete cover $= 3$ in

Core area, A_{core} = 324 in.^{2}

Spiral spacing, s = 1 in. (for steel and CFRP spirals) or 1.5 in (for GFRP spiral), in the confinement provided at the pile top and the pile toe.

Core width, b_c = 18 in.

Yield strength of steel transverse reinforcement, $f_{yh} = 70$ ksi (ASTM A1064-18a)

Tensile strength of bent FRP bars, $f_{fb} = \left(0.05\frac{r_b}{d_b} + 0.3\right) f_{fu} \leq f_{fu}$ (ACI 440.1R-15)

Assumed curvature of bent stirrup bars, $\frac{r_b}{d_b} = 4.0$

Environmental reduction factor, $C_E = 1.0$ for internal CFRP spiral (AASHTO, 2018) or 0.7 for GFRP spiral assuming concrete exposure to earth and weather (ACI 440.1R-15).

Design tensile strength, $f_{fu} = C_E \times f_{fu}^*$

The guaranteed ultimate tensile strength, $f_{fu}^* = 361.9$ ksi (for 0.2Ø CFRP spiral) or 120 ksi (for #3 GFRP spiral), according to FDOT (2019)

According to Section 5.11.4.1.4 of AASHTO (2017), force equilibrium requires that the minimum total cross-sectional area in a direction for a square section be no less than Equation (*D.1*) and Equation (*D.2*). The results for the minimum areas are summarized in Table D.1.

$$A_{sh} = 0.3sb_c\frac{f'_c}{f_{yh}}\left(\frac{A_g}{A_c} - 1\right) \quad \text{(D.1)}$$

$$A_{sh} = 0.12 s b_c \frac{f_c'}{f_{yh}} \tag{D.2}$$

Table D.1: AASHTO requirement for the required total cross sectional area A_{sh} of transverse reinforcement in the direction considered.

Spiral Type	A_{sh} in.^{2}
Steel	0.357
CFRP	0.138
GFRP	0.893

f_{yh} in Equation *(D.1)* and Equation *(D.2)*.were replaced by the bent strength, f_{fb}, of CRFP or GFRP transverse reinforcement.

For a square transverse reinforcement A_{sh}= $2A_{sp}$. Table D.2 shows the resulting required reinforcement area (A_{sp}) and diameter (d_{sp}). The bar diameters in Table D.2 suggest that Equation (*D.1*) and Equation (*D.2*) are applicable to piles in seismic regions only, and therefore cannot be used to predict or verify the requires spiral sizes in this project.

Table D.2: Required area of transverse reinforcements based on AASHTO equations

Spiral Type	A_{sp} in.^{2}	d_{sp} in.
Steel	0.178	0.48
CFRP	0.069	0.30
GFRP	0.447	0.75

Appendix E Prestress Loss Calculations

Strand properties

Elastic modulus of strand, $E_{ps} = 28500000$ psi

Area of one strand, $A_{strand} = 0.167$ in.^{2} (0.5" ϕ (special) Grade 270 Low-lax strand)

Guaranteed ultimate strength of strand, GUTS $= 270000$ psi

Number of strands $= 20$

Initial prestress in each of the 20 strands, $f_{pi} = 202500$ psi (75% of GUTS)

Initial force in each of the 20 strands, $P_i = 33.82$ kips

Concrete properties

$f'_{ci} = 4000$ psi (at 24 hours)

$$E_{ci} = 57000\sqrt{f'_{ci}} = 3604996 \text{ psi}$$

$f'_c = 6000$ psi (at 28 days)

$E_c = 57000\sqrt{f'_c} = 4415201$ psi

Length of pile, $L = 360$ in.

Losses due to elastic shortening of concrete (**ES**):

$$ES = \frac{K_{es} E_{ps} f_{cir}}{E_{ci}} \qquad \text{(E.1)}$$

where:

K_{es} =1.0 for pretensioned components

E_{ps} = modulus of elasticity of prestressing strands (28.5×10^6 psi)

E_{ci} = modulus of elasticity of concrete at time prestress is applied, psi

f_{cir} = net compressive stress in concrete at center of gravity of prestressing force immediately after the prestress has been applied to the concrete, psi:

$$f_{cir} = k_{cir}\left(\frac{P_i}{A_g} + \frac{P_i e^2}{I_g}\right) - \frac{M_g e}{I_g} \qquad \text{(E.2)}$$

where:

k_{cir} = 0.9 for pretensioned components

P_i = initial prestress force, lb.

e = eccentricity of center of gravity of tendons with respect to center of gravity of concrete at the cross section considered, in.

A_g = area of gross concrete section at the cross section considered, in.^{2}

I_g = moment of inertia of gross concrete section at the cross section considered, in.^{4}

M_g = bending moment due to dead weight of prestressed component and any other permanent loads in place at time of prestressing, lb.-in.

Therefore,

K_{es} =1.0

$k_{cir} = 0.9$

$P_i = 33.82$ kips

$e = 0$

$A_g = 574$ in.^{2}

$I_g = 27647.7$ in.^{4}

$M_g = 0$

$f_{cir} = 1060.48$ psi

$\mathbf{ES = 8383\ psi}$ (for each of the 20 strands)

Losses due to creep of concrete (CR):

$$\mathrm{CR} = \mathrm{k_{cr}}\left(\frac{\mathrm{E_{ps}}}{\mathrm{E_c}}\right)(\mathrm{f_{cir}} - \mathrm{f_{cds}}) \tag{E.3}$$

where:

$\mathrm{k_{cr}}$ = 2.0 for normal weight concrete and 1.6 for sand-lightweight concrete

$\mathrm{E_c}$ = modulus of elasticity of concrete at 28 days, psi

$\mathrm{f_{cds}}$ = stress in concrete at center of gravity of prestressing force due to all superimposed, permanent dead loads that are applied to the member after it has been prestressed, psi

$$\mathrm{f_{cds}} = \frac{\mathrm{M_{sd}}(\mathrm{e})}{\mathrm{I_g}} \tag{E.4}$$

where:

$\mathrm{M_{sd}}$ = moment due to all superimposed, permanent dead load and sustained load applied after prestressing, lb.-in.

Therefore,

$\mathrm{k_{cr}} = 2$

$\mathrm{f_{cds}} = 0$ (no eccentricity)

$\mathbf{CR = 13690\ psi}$

Losses due to shrinkage of concrete (SH):

$$\mathrm{SH} = (8.2 \times 10^{-6})\mathrm{K_{sh}}\mathrm{E_{ps}}\left(1 - 0.06\frac{\mathrm{V}}{\mathrm{S}}\right)(100 - \mathrm{RH}) \tag{E.5}$$

where:

$\mathrm{K_{sh}}$ = 1.0 for pretensioned components

$\frac{\mathrm{V}}{\mathrm{S}}$ = volume-to-surface ratio

RH = average ambient relative humidity (given in Design Aid 4.11.12 of PCI (2010)).

Therefore,

$K_{sh} = 1.0$

$V = A_g \times L = 206640 \text{ in.}^3$

$S = 36860 \text{ in.}^2$

$\frac{V}{S} = 5.61 \text{ in}$

$RH = 75\ \%$

$\mathbf{SH = 3877\ psi}$

Losses due to relaxation of strands (RE):

$$RE = [K_{re} - J(SH + CR + ES)]C \tag{E.6}$$

where:

Values for K_{re} and J are obtained from Table 5.7.1 of PCI (2010), and for values of coefficient C see Table 5.7.2 of PCI (2010).

$C = \left[\left(\frac{f_{pi}}{f_{pu}}\right)/0.21\right]\left[\left(\left(\frac{f_{pi}}{f_{pu}}\right)/0.9\right) - 0.55\right]$ for $\left(\frac{f_{pi}}{f_{pu}}\right) > 0.54$

$C = \left(\frac{f_{pi}}{f_{pu}}\right)/4.25$ for $\left(\frac{f_{pi}}{f_{pu}}\right) < 0.54$

$K_{re} = 5000$ (taken from Table 5.7.1 of PCI (2010))

$J = 0.04$ (taken from Table 5.7.1 of PCI (2010))

$SH + CR + ES = 25951 \text{ psi}$

ultimate strength of prestressing, $f_{pu} = 270000 \text{ psi}$

$f_{pi} = 202500 \text{ psi}$

$\frac{f_{pi}}{f_{pu}} = 0.750$

$\mathrm{C} = 1.012$

$\mathbf{RE = 4009\ psi}$

Total prestress losses, $(\mathbf{TL})$:

$$\mathrm{TL} = \mathrm{ES} + \mathrm{CR} + \mathrm{SH} + \mathrm{RE} \qquad \text{(E.7)}$$

$\mathbf{TL = 29960\ psi}$

Percentage prestress loss, TL $\% = \frac{\mathbf{TL}}{\mathbf{f_{pi}}} \times \mathbf{100} = \mathbf{14.80}\ \%$

Stress in each strand after losses ($\mathbf{f_{ps}}$):

$$\mathrm{f_{ps}} = \mathrm{f_{pi}} - \mathrm{TL} \qquad \text{(E.8)}$$

$\mathrm{f_{ps}} = 172539$ psi

Force in each strand after losses, $\mathrm{P_{ps}} = \mathrm{f_{ps}} \times \mathrm{A_{strand}} = 28.81$ kips

---

Force equivalent to effective prestress, $\mathrm{P_e} = 20 \times \mathrm{P_{ps}}$

Compressive stress in pile due to effective prestress, $\mathrm{f_{pe}} = \left[\mathrm{P_e}/\mathrm{A_g}\right]$

Compressive stress in pile due to effective prestress, $\mathbf{f_{pe}} = \mathbf{1.004\ ksi}$

Appendix F Moment Capacity Calculations

24 in. × 24 in. pile with 20 0.5" ϕ (special) strands

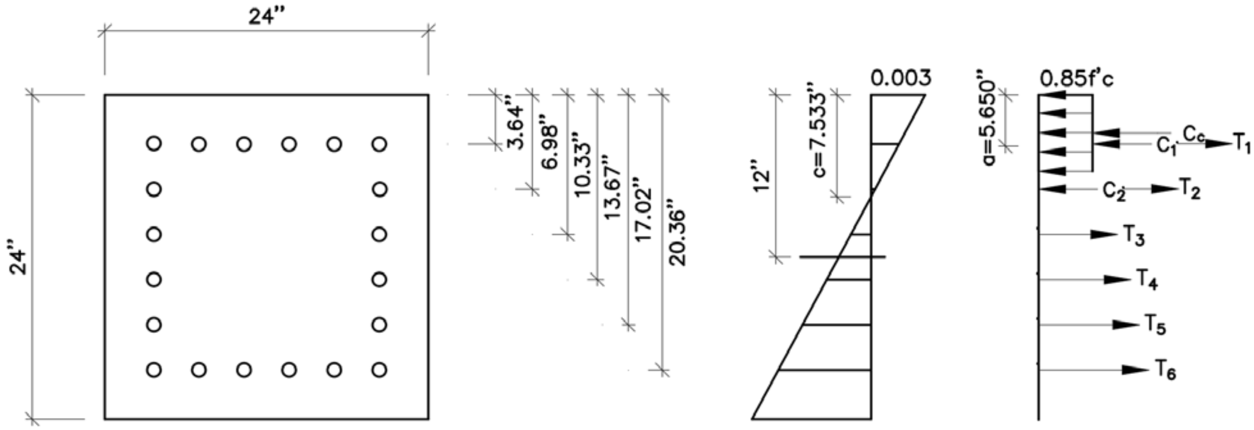

Parameters

$A_{strand} = 0.167 \text{ in.}^2$

$GUTS = 270 \text{ ksi}$

$f_{pi} = 202.5$ ksi (75% of GUTS)

$P_i = 33.82$ kips

Initial strain in strands, $\varepsilon_{psi} = 0.007105$ in./in.

$f'_{ci} = 6$ ksi (at 28 days)

$\beta_1 = 0.75$

Neutral axis, $c = 7.533$ in. (based on trials)

Stress block depth, $a = 5.650$ in.

Concrete strain limit, $\varepsilon_c = 0.003 \text{ in./in.}$

$E_{ps} = 28500 \text{ ksi}$

Pile width, $b = 24$ in.

Pile height, $h = 24$ in.

Force in concrete, C_c:

$$C_c = 0.85 f'_c ab \tag{F.1}$$

$C_c = -686.45$ kips (negative sign represents compression).

Concrete moment (taken about $\frac{h}{2}$), $M_c = 6298.15\ \text{kip} - \text{in}$

Force and moment due to prestressing strands:

f_{ps} = Effective stress in prestressing after losses

$\varepsilon_{ps} =$ Effective strain in prestressing after losses $= \frac{f_{ps}}{E_{ps}}$

ε_p = Strain in prestressing due to applied moment = $\varepsilon_c \left[\frac{d}{c} - 1\right]$

ε_{final} = Strain in prestressing due at ultimate moment = $\varepsilon_{ps} + \varepsilon_p$

f_{final} = Stress in the prestressing at ultimate moment = $E_{ps} \times \varepsilon_{final}$ or $270 - \left[\frac{0.004}{\varepsilon_{final} - 0.007}\right]$ for $\varepsilon_{final} > 0.0085$ (Design Aid 15.3.3 of PCI (2010))

$F_{strands}$ = Force in prestressing at ultimate moment = Number of strands per layer $\times A_{strand} \times f_{final}$

Table F.1: Strand moment calculation

Nominal initial force (kips)	**No of strands per layer**	**A_{strand} (in.^{2})**	**d_p (in)**	**f_{ps} (ksi)**	**ε_{ps} (in./in.)**	**ε_p (in./in.)**	**ε_{final} (in./in.)**	**f_{final} (ksi)**	**$F_{strands}$ (kips)**	**subtract force if strand is in comp (kips)**	**$F_{strands}$ minus holes (kip)**	**M_{ps} about h/2 (kip-in)**
33.82	6	1.002	3.64	172.54	0.00605	-0.00155	0.00450	128.35	128.61	-5.11	133.72	-1117.89
33.82	2	0.334	6.98	172.54	0.00605	0.00022	0.00583	166.26	55.53	-1.70	57.23	-287.31
33.82	2	0.334	10.33	172.54	0.00605	0.00111	0.00717	204.28	68.23	0.00	68.23	-113.94
33.82	2	0.334	13.67	172.54	0.00605	0.00244	0.00850	242.19	80.89	0.00	80.89	135.09
33.82	2	0.334	17.02	172.54	0.00605	0.00378	0.00983	255.88	85.46	0.00	85.46	429.02
33.82	6	1.002	20.36	172.54	0.00605	0.00511	0.01116	260.39	260.91	0.00	260.91	2181.21
											686.45	1226.17

Sum of forces = $C_c + F_{strands} = 0.00$ kips

Nominal moment, $\mathbf{M_n = M_c + M_{ps} = 7524.32\ kip - in}$

Appendix G Calculations for Axial Capacities and Compression Driving Stress Limits

Parameters

$f'_c(\text{at 28 days}) = 6000\ \text{psi}$

$A_g = 574\ \text{in.}^2$

$f_{pe} = 1.004\ \text{ksi}$

Allowable service axial capacity, N:

$$N = (0.33f'_c - 0.27f_{pe})A_g \text{ (according to PCI (1999, 2010))} \tag{G.1}$$

$N = 980.92\ \text{kips}$

Nominal axial load capacity, P_o:

$$P_o = (0.85f'_c - 0.6f_{pe})A_g \text{ (according to PCI (1999))} \tag{G.2}$$

$P_o = 2581.62\ \text{kips}$

The maximum allowable driving stresses (compression stress limits):

$$S_{apc-AASHTO} = (0.85f'_c - f_{pe}) \text{ (AASHTO (2017) compression driving stress limit)} \tag{G.3}$$

$S_{apc-AASHTO} = 4.10\ \text{ksi}$

$$S_{apc-FDOT} = (0.7f'_c - 0.75f_{pe}) \quad \text{(FDOT (2019) compression driving stress limit)} \tag{G.4}$$

$S_{apc-FDOT} = 3.45\ \text{ksi}$

The maximum allowable driving stresses (tension stress limits):

$S_{apt-AASHTO} = 0.095\sqrt{f'_c} + f_{pe}$ (AASHTO (2017) tension driving stress limit in normal environment, ksi) $= 1.24$ ksi (G.5)

$S_{apt-AASHTO} = f_{pe}$ (AASHTO (2017) tension driving stress limit in corrosive environment, ksi) $= 1.00$ ksi (G.6)

$$S_{apt-FDOT} = 6.5(f'_c)^{0.5} + 1.05f_{cpe} \text{ (FDOT (2019) tension driving stress limit in psi)} \tag{G.7}$$

where

f_{cpe} = effective prestress (after all losses) at the time of driving, psi, taken as 0.8 times the initial prestress force divided by the minimum net concrete cross-sectional area of the pile

$f_{cpe} = \frac{0.8 \times P_i \times 20}{A_g} = 942.65 \text{ psi}$

$S_{apt-FDOT} = 1.49 \text{ ksi}$

Equivalent force for the maximum allowable driving stresses (Compression stress limits):

$P_{AASHTO} = S_{apc-AASHTO} \times A_g = 2351.10 \text{ kips}$

$P_{FDOT} = S_{apc-FDOT} \times A_g = 1978.58 \text{ kips}$

Appendix H Calculations for Flexural Displacement

Cracked moment of inertia:

Parameters

$A_{strand} = 0.167$ in.^{2}

Total area of prestressing strands, $A_{ps} = 3.34$ in.^{2}

$E_{ps} = 28500$ ksi

$f'_{ci} = 6$ ksi (at 28 days)

$E_c = 4415.20$ ksi

Modular ratio, $n = \frac{E_{ps}}{E_c} = 6.45$

c' (neutral axis of cracked transformed section) $= 3.82$ in.

Distance from center of gravity of prestressing in compression zone to the extreme compression fiber $= d'$ (see Table H.1)

Distance from center of gravity of prestressing in tension zone to the extreme compression fiber$=$ d (see Table H.1)

Area of concrete in the compression zone $= A_c$

Area of strands in each layer $= A_s$

The cracked moment of inertia, I_{cr}:

$$I_{cr} = \frac{bc'^3}{12} + A_c(d - c')^2 + nA_s(d - c')^2 + nA_s - A_s(c' - d')^2 \quad \text{(H.1)}$$

Table H.1: Cracked moment of inertia calculation

	Area (A_c *or* A_s) (in.^{2})	$c'/2$ (in.^{2})	d' or d (in.)	I (in.^{4})	$A_c(d-c')^2$ (in.^{4})	$nA_s(d-c')^2$ (in.^{4})	$nA_s - A_s(c'-d')^2$ (in.^{4})	I_{cr} (in.^{4})
Conc in compression	90.68	1.91	–	111.49	330.81	–	–	–
Strand in tension zone, T_3	0.33	–	10.33	–	–	91.37	–	–
Strand in tension zone, T_4	0.33	–	13.67	–	–	209.18	–	–
Strand in tension zone, T_5	0.33	–	17.02	–	–	375.65	–	–
Strand in tension zone, T_6	1.00	–	20.36	–	–	1769.43	–	–
Strand in comp zone, T_1	1.00	–	3.64	–	–	–	0.18	
Strand in comp zone, T_2	0.33	–	6.98	–	–	–	18.19	–
				111.49	330.81	2445.63	18.37	**2906.30**

Parameters for the calculation of flexural displacement

$f'_c = 6$ ksi (at 28 days)

$E_c = 4415.20$ ksi

$A_{ps} = 3.34$ in.^{2}

Longitudinal reinforcement ratio, $\rho_{ps} = \frac{A_{ps}}{bh} = 0.006$

Modular ratio, $n = \frac{E_{ps}}{E_c} = 6.45$

Pile length $= 30$ ft. $=$ 360 in

Span length, L (between supports) $= 28$ ft. $=$ 336 in.

Distance between the center line of support and the first load point, $\mathrm{X} = 11\ \mathrm{ft.} = 132\ \mathrm{in.}$

Self-weight of pile, $\mathrm{w_g} = \mathrm{A_g} \times 150 \frac{\mathrm{lb}}{\mathrm{ft.}^3} = 0.598 \frac{\mathrm{kip}}{\mathrm{ft.}} = 0.050 \frac{\mathrm{kip}}{\mathrm{in.}}$

Moment due to self-weight, $\mathrm{M_g} = \frac{\mathrm{w_g L^2}}{8} = 703\ \mathrm{kip - in.}$

Failure actuator load:

Failure load 1 (actuator load + load from spreader beam and pile self-weight), $\mathrm{P_{d1}} = \left(\frac{\mathrm{M_n}}{\mathrm{X}}\right) 2 = \left(\frac{7524}{132}\right) 2 = 114\ \mathrm{kips}$

Failure load 2 (actuator load + load from spreader beam), $\mathrm{P_{d2}} = \left(\frac{\mathrm{M_n - M_g}}{\mathrm{X}}\right) 2 = 103.35\ \mathrm{kips}$

Failure actuator load, $\mathbf{P_{act} = 102.35\ kips}$ (taking the weight of the spreader beam as 1 kip)

Cracking moment of pile and actuator load at cracking, $\mathbf{M_{cr}}$ and $\mathbf{P_{cr-act}}$:

$$\mathrm{M_{cr}} = \frac{(\mathrm{f_r + f_{pe} - f_d})\mathrm{I_g}}{\mathrm{y_t}} \text{ (Hawkins et al. (2005) and Article 24.2.3.9 of (ACI 318-14))} \tag{H.2}$$

where

Tensile strength of concrete, $\mathrm{f_r} = 0.24\sqrt{\mathrm{f'_c}} = 0.588\ \mathrm{ksi}$ (Article 5.4.2.6 of AASHTO (2017))

Compressive stress due to effective, $\mathrm{f_{pe}} = \frac{\mathrm{P_e}}{\mathrm{A_g}} = 1.004\ \mathrm{ksi}$

Stress due to unfactored dead load (self-weight), $\mathrm{f_d} = \frac{\mathrm{M_g}}{\mathrm{I_g / y_t}}$

$\mathrm{I_g} = 27647.7\ \mathrm{in.}^4$

Distance from the neutral axis to the extreme tension fiber of uncracked section, $\mathrm{y_t} = 12\ \mathrm{in.}$

$\mathbf{M_{cr} = 2964.43\ kip - in.}$

Cracking load 1 (actuator load + load from spreader beam and pile self-weight), $\mathrm{P_{cr1}} = \left(\frac{\mathrm{M_{cr}}}{\mathrm{X}}\right) 2 = \left(\frac{2964}{132}\right) 2 = 44.92\ \mathrm{kips}$

Cracking load 2 (actuator load + load from spreader beam), $\mathrm{P_{cr2}} = \left(\frac{\mathrm{M_{cr} - M_g}}{\mathrm{X}}\right) 2 = 34.26\ \mathrm{kips}$

Cracking actuator load, $\mathbf{P_{cr-act} = 33.26\ kips}$ (taking the weight of the spreader beam as 1 kip)

Effective moment of inertia, $\mathbf{I_e}$:

$$I_e = \left(\frac{M_{cr}}{M_a}\right)^3 I_g + \left[1 - \left(\left(\frac{M_{cr}}{M_a}\right)^3\right)\right] I_{cr} \text{ (Article 5.6.3.5 of AASHTO (2017))} \qquad \text{(H.3)}$$

where

Maximum moment in a component at the stage for which deformation is computed, $M_a = 7524.32$ kip − in (taken as moment when moment capacity is reached)

Cracked moment of inertia, $I_{cr} = 2906$ in.^{4}

$\mathbf{I_e = 4419.33\ in.^4}$

Displacement:

$\delta = \left[\frac{5w_g L^4}{384\mathbf{E_c I_g}}\right] + \left[\frac{\mathbf{P_{d1}X}(3L^2 - 4X^2)}{48\mathbf{E_c I_e}}\right] = 4.39$ in (displacement due to self-weight + displacement due to applied load)

$\delta_{act} = \left[\frac{\mathbf{P_{act}X}(3L^2 - 4X^2)}{48\mathbf{E_c I_e}}\right] = 3.88$ in (displacement due to actuator load)

Appendix I Calculations for Shear Capacity of Transverse Reinforcement

The nominal shear resistance, V_n:

$$V_n = \min\left(\left(V_c + V_s + V_p\right), \left(0.25f'_c b_v d_v + V_p\right)\right) \quad \text{(I.1)}$$

where

V_c = concrete contribution to nominal shear resistance

V_s = transverse reinforcement contribution to nominal shear resistance

V_p = nominal shear resistance from prestressing (= 0 for straight strands)

d_v = effective shear depth = max $\left(d_e - \frac{a}{2},\ 0.9d_e,\ 0.72h\right)$

$d_v = \max(9.18\text{ in.}, 10.8\text{ in.}, 17.3\text{ in.})$

$$d_e = \frac{A_s f_y d_p + A_{sp} f_{sp} d_p}{A_s f_y + A_{sp} f_{sp}}$$

Note: $A_s f_y$ applies to non-prestressed steel reinforcement, which is taken as zero in this calculation.

b_v = effective width = b_w

$f'_c = 6$ ksi

Concrete contribution to nominal shear resistance, V_c:

$$V_c = \min\left(V_{ci}, V_{cw}\right) \text{ (Hawkins et al. (2005))} \quad \text{(I.2)}$$

where

V_{ci} = nominal shear resistance provided by concrete when inclined cracking results from combined shear and moment (flexure shear) = $0.02\sqrt{f'_c}\,b_v d_v + V_d + \frac{V_i M_{cr}}{M_{max}}$

V_{cw} = nominal shear resistance provided by concrete when inclined cracking results from excessive principal tensions in web (web shear) = $(0.06\sqrt{f'_c} + 0.30f_{pc})b_v d_v + V_p$

V_d = shear force at section due to unfactored dead load

V_i = factored shear force at section due to externally applied loads occurring simultaneously with M_{max}

M_{cr} = moment causing flexural cracking at section due to externally applied loads

M_{max} = maximum factored moment at section due to externally applied loads

f_{pc} = compressive stress in concrete after allowance for all prestress losses at centroid of cross section

V_c =73.44 kips

Transverse reinforcement contribution to nominal shear resistance, V_s:

The following shows the calculation of V_s for a steel spiral in a standard 24-inch square prestressed concrete pile.

$V_s = \frac{A_v f_y d_v \cot(\theta)}{s}$ (Equation C5.8.3.3-1 of AASHTO (2012)) (I.3)

where

s = spacing of transverse reinforcement (taken at largest spacing along the pile) = 6 in

A_v = area of all vertical legs of stirrup = $2 \times$ area of transverse reinforcement = $2 \times 0.034 = 0.068\ \text{in.}^2$

θ = angle of inclination for diagonal compressive stresses

$\cot(\theta) = \min\left[1 + 3\left(\frac{f_{pc}}{\sqrt{f'_c}}\right),\ 1.8\right]$ if $V_{ci} > V_{cw}$, $\cot(\theta) = 1$ $V_{ci} < V_{cw}$ (Article 5.8.3.4.3 of AASHTO (2012))

From excel calculations $V_{ci} < V_{cw}$

V_s =13.71 kips

Therefore $V_n = V_c + V_s$ =87.15 kips (for pile with steel spiral)

Selection of GFRP transverse reinforcement

The aim here is to determine which GFRP rebar provides similar shear resistance to the shear resistance calculated for the steel spiral as described above.

Trial #1

Try #2 GFRP rebar.

Bar diameter, $d_b = 0.25$ in.

Area of FRP bar, $A_f = 0.049\ \text{in.}^2$

Area of shear reinforcement, $A_{fv} = 2 \times A_f = 0.098\ \text{in.}^2$

The guaranteed ultimate tensile load, $F_{fu}{}^* = 6.10$ kips (FDOT (2019))

The guaranteed ultimate tensile strength, $f_{fu}{}^* = 124.49$ ksi

Modulus of elasticity, $E_{GFRP} = 6500$ ksi (ASTM D7957-17)

Design material properties:

Environmental reduction factor, $C_E = 0.7$ (Table 6.2, ACI 440.1R-15)

Design tensile strength, $f_{fu} = C_E \times f_{fu}{}^* = 87.14$ ksi

Assumed curvature of bent stirrup bars, $\frac{r_b}{d_b} = 4.0$

r_b = bend radius of the bar

d_v = effective depth = 17.28 in.

Determine design tensile stress in transverse reinforcement.

a. Based on tensile strength of bent bars, $f_{fb} = \left(0.05\frac{r_b}{d_b} + 0.3\right) f_{fu} \leq f_{fu}$ (ACI 440.1R-15)

   $f_{fb} = 43.57$ ksi

b. Tensile strength based on a tensile strain limit (0.004) for a conservative prediction of tensile strength (ACI 440.1R-15)

$f_{fv} = 0.004E_{GFRP} \leq f_{fu}$

$$f_{fv} = 26 \text{ ksi}$$

Determine shear resistance.

For FRP rectangular spirals, the shear contribution, $V_f = \frac{A_{fv}f_{fv}d_v\cot(\theta)}{s}$ (CSA-806)

s = spiral pitch (taken at largest spacing along the pile) $= 6$ in

a. Based on tensile strength of bent bars, f_{fb}

$$V_{fb} = \frac{A_{fv}f_{fb}d_v\cot(\theta)}{s} = 12.30 \text{ kips}$$

b. Based on tensile strain limit (0.004)

$$V_f = \frac{A_{fv}f_{fv}d_v\cot(\theta)}{s} = 7.34 \text{ kips}$$

V_{fb} and V_f are less thn V_s=13.71, #2 GFRP rebar is inadequate.

Trial #2

Try #3 GFRP rebar.

Bar diameter, $d_b = 0.375$ in.

Area of FRP bar, $A_f = 0.11 \text{ in.}^2$

Area of shear reinforcement, $A_{fv} = 2 \times A_f = 0.22 \text{ in.}^2$

The guaranteed ultimate tensile load, $F_{fu}{}^* = 13.20$ kips (FDOT (2019))

The guaranteed ultimate tensile strength, $f_{fu}{}^* = 120$ ksi

Modulus of elasticity, $E_{GFRP} = 6500$ ksi (ASTM D7957-17)

Design material properties:

Environmental reduction factor, $C_E = 0.7$ (Table 6.2, ACI 440.1R-15)

Design tensile strength, $f_{fu} = C_E \times f_{fu}^* = 84$ ksi

Assumed curvature of bent stirrup bars, $\frac{r_b}{d_b} = 4.0$

r_b = bend radius of the bar

d_v = effective depth $= 17.28$ in.

Determine design tensile stress in transverse reinforcement

a. Based on tensile strength of bent bars, $f_{fb} = \left(0.05\frac{r_b}{d_b} + 0.3\right) f_{fu} \leq f_{fu}$ (ACI 440.1R-15)

$$f_{fb} = 42 \text{ ksi}$$

b. Tensile strength based on a tensile strain limit (0.004) for a conservative prediction of tensile strength (ACI 440.1R-15)

$f_{fv} = 0.004E_{GFRP} \leq f_{fu}$

$f_{fv} = 26$ ksi

Determine shear resistance.

For FRP rectangular spirals, the shear contribution, $V_f = \frac{A_{fv} f_{fv} d_v \cot(\theta)}{s}$ (CSA-806)

s = spiral pitch (taken at largest spacing along the pile) $= 6$ in.

θ = angle of inclination of diagonal compressive stresses

a. Based on tensile strength of bent bars, f_{fb}

$$V_{fb} = \frac{A_{fv} f_{fb} d_v \cot(\theta)}{s} = 26.61\text{kips}$$

b. Based on tensile strain limit (0.004)

$$V_f = \frac{A_{fv} f_{fv} d_v \cot(\theta)}{s} = 16.47 \text{ kips}$$

V_f and V_{fb} are greater than $V_s = 13.71$ kips, #3 GFRP rebar is adequate.

Shear contribution from the 0.2”-diameter CFRP spiral from Roddenberry et al. (2014)

Bar diameter, $d_b = 0.2$ in.

Area of FRP bar, $A_f = 0.0236$ in.^{2}

Area of shear reinforcement, $A_{fv} = 2 \times A_f = 0.0472 \text{ in.}^2$

The guaranteed ultimate tensile load, $F_{fu}{}^* = 8.54$ kips

The guaranteed ultimate tensile strength, $f_{fu}{}^* = 361.9$ ksi

Modulus of elasticity, $E_{CFRP} = 22400$ ksi (pending requirements in FDOT specifications 932-3)

Design material properties:

Environmental reduction factor, $C_E = 1$ (AASHTO, 2018)

Design tensile strength, $f_{fu} = C_E \times f_{fu}{}^* = 361.9$ ksi

Assumed curvature of bent stirrup bars, $\frac{r_b}{d_b} = 4.0$

r_b = bend radius of the bar

d_v = effective depth = 17.28 in.

Determine design tensile stress in shear reinforcement.

a. Tensile strength based on a tensile strain limit (0.004) for a conservative prediction of tensile strength (ACI 440.1R-15)

   $f_{fv} = 0.004E_{GFRP} \leq f_{fu}$

   $f_{fv} = 89.6$ ksi

b. Based on tensile strength of bent bars, $f_{fb} = \left(0.05\frac{r_b}{d_b} + 0.3\right) f_{fu} \leq f_{fu}$ (ACI 440.1R-15)

$$f_{fb} = 180.93 \text{ ksi}$$

Determine shear resistance.

For continuous FRP rectangular spirals, the shear contribution of FRP spirals, $V_f = \frac{A_{fv} f_{fv} d_v \cot(\theta)}{s}$ (CSA 806)

s = spiral pitch (taken at largest spacing along the pile) = 6 in

θ = angle of inclination for diagonal compressive stresses

Conservative prediction based on tensile strain limit (0.004)

$$V_f = \frac{A_{fv} f_{fv} d_v \cot(\theta)}{s} = 12.18 \text{ kips}$$

c. Based on tensile strength of bent bars, f_{fb}

$$V_{fb} = \frac{A_{fv} f_{fb} d_v \cot(\theta)}{s} = 24.60 \text{ kips}$$

V_{fb} is greater than $V_s = 13.71$ kips, while V_f is less than V_s.